PUBLIC ROADS

A JOURNAL OF HIGHWAY RESEARCH

UNITED STATES DEPARTMENT OF AGRICULTURE
BUREAU OF PUBLIC ROADS

VOL. 9, NO. 11 ▽ JANUARY, 1929

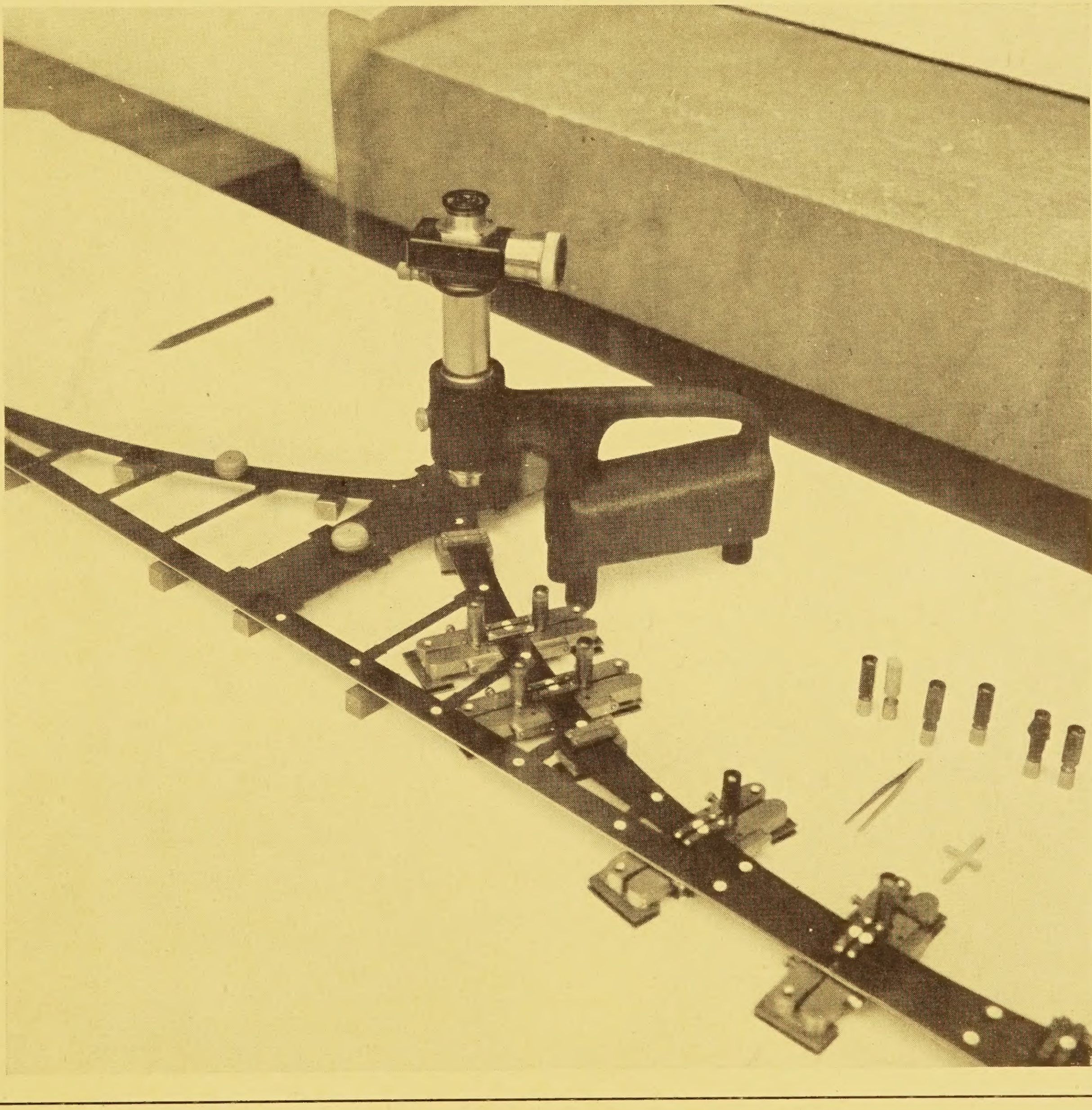

APPARATUS FOR MODEL ANALYSIS OF YADKIN RIVER BRIDGE

U. S. GOVERNMENT PRINTING OFFICE: 1929

PUBLIC ROADS

A JOURNAL OF HIGHWAY RESEARCH

U. S. DEPARTMENT OF AGRICULTURE

BUREAU OF PUBLIC ROADS

CERTIFICATE: By direction of the Secretary of Agriculture, the matter contained herein is published as administrative information and is required for the proper transaction of the public business

The reports of research published in this magazine are necessarily qualified by the conditions of the tests from which the data are obtained. Whenever it is deemed possible to do so, generalizations are drawn from the results of the tests; and, unless this is done the conclusions formulated must be considered as specifically pertinent only to the described conditions

VOL. 9, NO. 11 | JANUARY, 1929 | R. E. ROYALL, Editor

TABLE OF CONTENTS

THE U. S. BUREAU OF PUBLIC ROADS

Willard Building, Washington, D. C.

REGIONAL HEADQUARTERS

Mark Sheldon Building, San Francisco, Calif.

DISTRICT OFFICES

DISTRICT No. 1, Oregon, Washington, and Montana.
Box 3900, Portland, Oreg.

DISTRICT No. 2, California, Arizona, and Nevada.
Mark Sheldon Building, San Francisco, Calif.

DISTRICT No. 3, Colorado, New Mexico, and Wyoming.
301 Customhouse Building, Denver, Colo.

DISTRICT No. 4, Minnesota, North Dakota, South Dakota, and Wisconsin.
410 Hamm Building, St. Paul, Minn.

DISTRICT No. 5, Iowa, Kansas, Missouri, and Nebraska.
8th Floor, Saunders-Kennedy Bldg., Omaha, Nebr.

DISTRICT No. 6, Arkansas, Oklahoma, and Texas.
1912 Fort Worth National Bank Building, Fort Worth, Tex.

DISTRICT No. 7, Illinois, Indiana, Kentucky, and Michigan.
South Chicago Post Office Building, Chicago, Ill.

DISTRICT No. 8, Louisiana, Alabama, Georgia, Florida, Mississippi, South Carolina, and Tennessee.
Box J, Montgomery, Ala.

DISTRICT No. 9, Connecticut, Maine, Massachusetts, New Hampshire, New Jersey, New York, Rhode Island, and Vermont.
Federal Building, Troy, N. Y.

DISTRICT No. 10, Delaware, Maryland, North Carolina, Ohio, Pennsylvania, Virginia, and West Virginia.
Willard Building, Washington, D. C.

DISTRICT No. 11, Alaska.
Goldstein Building, Juneau, Alaska.

DISTRICT No. 12, Idaho and Utah.
Fred J. Kiesel Building, Ogden, Utah.

Owing to the necessarily limited edition of this publication it will be impossible to distribute it free to any persons or institutions other than State and county officials actually engaged in planning or constructing public highways, instructors in highway engineering, periodicals upon an exchange basis, and Members of both Houses of Congress. At the present time names can be added to the free list only as vacancies occur. Others desiring to obtain PUBLIC ROADS can do so by sending 10 cents for a single number or $1 per year to the Superintendent of Documents, U. S. Government Printing Office, Washington, D. C.

MODEL ANALYSIS OF A REINFORCED CONCRETE ARCH

REPORT ON A COOPERATIVE STUDY BY THE JOHNS HOPKINS UNIVERSITY AND UNITED STATES BUREAU OF PUBLIC ROADS IN CONNECTION WITH YADKIN RIVER BRIDGE TESTS

Reported by J. T. THOMPSON, Highway Research Specialist, Division of Tests, United States Bureau of Public Roads, and also Associate Professor of Civil Engineering, The Johns Hopkins University [1]

IN A PREVIOUS report [2] on the North Carolina bridge tests there was presented a comparison of the measured and computed deformations of a reinforced concrete arch bridge under live load with the deformations as determined by the use of an elastic model of sheet celluloid and Beggs deformeter gauges. In the previous report the model analysis was not discussed in detail and only the results were given.

During the progress of the analysis there arose some interesting problems in technique. It is believed that a detailed description of the procedure, an explanation of the problems encountered, and the manner in which these problems were solved will be helpful to those who meet with similar difficulties in using this method.

DEFORMETER METHOD DESCRIBED

Professor Beggs has described the principle and operation of his deformeter method elsewhere,[3] but a brief description will be undertaken here for the sake of those who are unfamiliar with it.

Suppose it is desired to determine the thrusts, shears, and moments in the arch rib of a structure, the model of which is shown in Figure 1. The model is prepared from a sheet of celluloid approximately one-tenth of an inch thick, the sectional dimensions of the model being proportional to the cube roots of the moments of inertia of the various sections of the actual structure according to some convenient scale. If we wish to determine the thrust at M, for example, due to a vertical load of unity at 4, we can do so by cutting the arch rib at M normal to the rib axis and separating the sides of the cut a small known distance d_1, care being taken to keep the sides of the cut parallel. This displacement of the sides of the cut produces distortions throughout the model, and if we measure with a microscope the resulting vertical deflection d_2 at 4, we have all the data necessary for computing the thrust T at M. It follows from the Maxwell theorem of reciprocal deflections that for a unit load, $I = \frac{d_2}{d_1}$. It is necessary, of course, that d_1, and d_2 be measured in the same units (say inches) and this is accomplished by multiplying an observed deflection by the calibration factor of the microscope. It is obvious that if similar measurements are made of the vertical deflections at points 0 to 6 due to the displacement of the cut section M, an influence curve can be plotted for the thrust at M.

By the same reasoning an influence diagram for the the shear at M can be determined by measuring the vertical deflections at points 0 to 6 due to a small known shear displacement of the sides of the cut section.

Likewise if the two sides of the cut section are rotated with respect to one another through a small known angle and the necessary measurements of deflections made, an influence diagram for bending moment at M can be plotted, the only difference being that in the case of moments the scale of the model plays a part; it is necessary to multiply the deflections d_2 by the scale of the model. For example if the scale of the model is 1 inch to 5 feet, all observed deflections must be multiplied by 5, to obtain the moment in foot-pounds. That is, the deflections d_2 for a given angular rotation in the model must be multiplied by the value of a unit length of the model in the actual structure to obtain the deflection in the actual structure for the same rotation. In the example given the model deflections would be multiplied by 60 to obtain the moment in inch-pounds due to a load of one pound and by 5 to obtain the moment in foot-pounds.

The foregoing paragraphs set forth the principle upon which the Beggs method is based. In practice the displacements of the sides of the cut section are

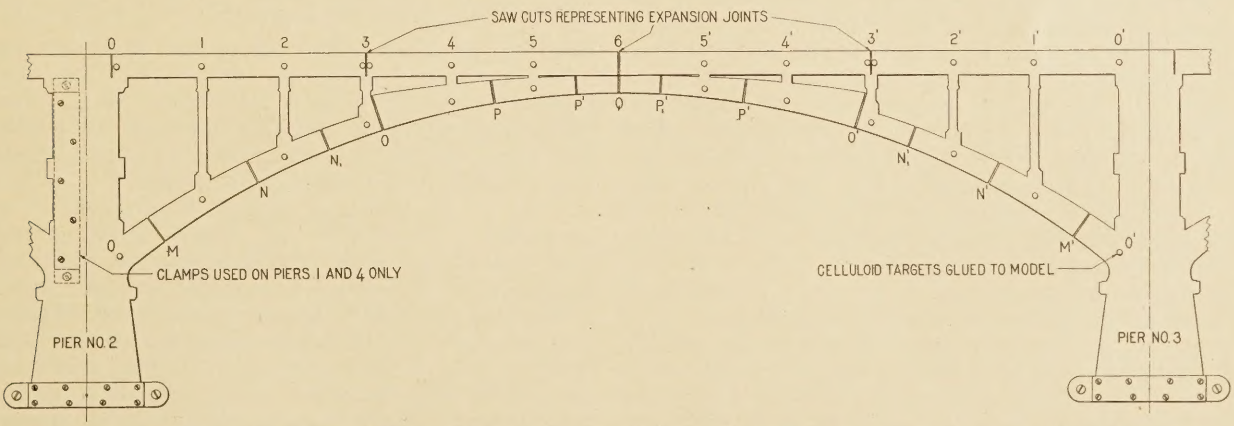

FIG. 1.—OUTLINE OF MODEL OF YADKIN RIVER BRIDGE SHOWING SECTIONS AT WHICH GAUGES WERE ATTACHED

[1] The analysis was made at the Johns Hopkins University by the author and Albin L. Gemeny, Senior Structural Engineer of the Bureau of Public Roads.
[2] Gemeny, A. L. and Hunter, W. F., Loading Tests on a Reinforced Concrete Arch, Public Roads, vol. 9. No. 10, December 1928.
[3] Beggs, George., The use of Models in the Solution of Indeterminate Structures, Journal of the Franklin Institute, March, 1927.

brought about by means of a deformeter gauge and plugs which are inserted therein. The gauge (fig. 2) consists of two steel bars drawn toward each other by springs. In the opposing sides of these bars are notches into which the plugs are inserted. The model is first attached to a drawing board by clamps attached at points of fixity in the actual structure such as the bases of piers, etc. The underside of the model lies in a plane five-eighths inch from the drawing board and is supported at numerous points upon ½-inch blocks of glass or metal and ⅛-inch steel ball bearings. The gauge is attached to the model, normal to the axis along which the thrust acts and is supported upon two $\frac{1}{16}$-inch plates between which three ⅛-inch steel ball bearings have been placed. Two normal plugs, midway in size between the large and small thrust plugs, are inserted before the gauge clamps are tightened. After screwing the clamps down tightly against the model the normal plugs are removed and the model cut through with a hack-saw blade. Thereafter, whenever the normal plugs are inserted the model resumes exactly the position it was in before the section was cut.

Thrust measurements are made by inserting first the two exactly similar small-size thrust plugs, reading the microscopes, which are of the filar micrometer type, and then inserting the large-size thrust plugs and again reading the microscopes. The microscopes are so oriented that vertical deflections are recorded by them and the differences in settings are the deflections d_2.

Shear displacements are produced by inserting the shear plugs, which are also exactly alike, with the flat portion bearing first against the faces, 1, of the notches and then against the faces, 2. This causes one side of the gauge to be displaced laterally with respect to the other side, the sides of the cut section remaining parallel and exactly the same distance apart as when the normal plugs are in place. The moment displacements are produced by inserting the two moment plugs, which are of different diameters, and then interchanging them.

CELLULOID MODEL CONSTRUCTED

In making the model of the Yadkin River Bridge the total moment of inertia of the concrete plus n times the moment of inertia of the steel was first computed for each of the various sections of the actual structure and the sectional dimensions of the model were based on the cube roots of these quantities. The scale of these sectional dimensions was selected so that the width of the arch rib did not, in general, exceed a size that could be grasped by the clamps on the gauges. This resulted in the selection of 1 inch to 5 feet as the proper scale, and a model approximately 100 inches long, since the bridge consisted of three equal arches of approximately 150 feet clear span each, a total of about 500 feet from end to end.

The outline of one-half of the model was next carefully scribed on a thin sheet of aluminum and small holes drilled at frequent intervals along the scribed lines. This templet was then clamped to a sheet of 0.08-inch celluloid, 20 by 50 inches in size, and center punch marks were made through the holes drilled in the templet. These punch marks were later used in scratching the outline of the model on the celluloid. The templet was next clamped to a new position on the celluloid sheet and the process repeated. By taking advantage of the symmetry of the structure, much labor was saved in laying out the model on the celluloid and mistakes which would no doubt have been made in scratching directly on the celluloid were avoided. The two halves of the model were roughly sawed out with a coping saw and filed down to the outlines.

CARE USED IN SETTING UP MODEL TO PRODUCE ACCURATE RESULTS

In mounting the model upon the drawing board a finishing nail was driven just beyond each end of the model and a cotton thread stretched taut between them. The two halves of the model were then placed in approximate position and supported upon ⅛-inch steel ball bearings which rested in turn upon ½-inch brass blocks. The top of the model was adjusted to the cotton thread reference line and the bottoms of the four piers were clamped to the board. A gauge was placed at the crown connecting the two halves of the model. In order to simulate the condition of restraint offered by the approach spans, the two end piers of the model were also fastened with the clamps shown in Figure 1.

The reference line formed by the cotton thread proved of considerable value not only in setting the two halves of the arch in position but also in indicating the normal position of the model throughout the analysis.

In order to increase the ease and accuracy of microscope reading, targets were glued to the model at points where microscope readings were to be taken. These targets consisted of small disks punched from a sheet of white celluloid. The point to be observed on the disk was indicated by making a very small indentation with the point of a fine needle and then smearing a little India ink over the target. When the surplus ink was wiped off some of it remained in the indentation, producing a very small, round speck in striking contrast with the white celluloid background.

In making the field tests, stresses were measured by telemeters in both the extrados and intrados of the central arch at points M, N, O, P, Q, P′, O′, N′, and M′ indicated in Figure 1. It was necessary, therefore, in order to check these stresses, to attach gauges at those points. The other field results with which it was desired to compare results from the model analysis were the rotations at nine points of the arch axis which had been measured in the field with clinometers Since these rotations $\Sigma\frac{Mds}{EI}$ are dependent upon the bending moments in the rib, it was necessary to draw a bending-moment diagram for the rib. This obviously made it necessary to have deformeter data from each panel from which to compute the bending moments at the sides of the columns. Accordingly gauges were also attached at points N_1, N'_1, P_1, and P'_1. This made a total of 13 points at which deformeter data were necessary. Since only six gauges were available, it was necessary, after the first six points had been investigated, to remove the gauges to other points.

The cut sections, left upon the removal of the gauges had, of course, to be repaired in some way. Although welding with a thick solution of celluloid in acetone is commonly recommended for this purpose, tests, made in advance, indicated that about 48 hours must elapse before the welded section becomes hard and elastic. Small clamps were therefore used in order to save time. These clamps consisted of small brass blocks, ¾ by 1¼ by $\frac{7}{16}$ inches, with straps similar to those on the deformeter gauges. The two sides of the cut were clamped down to the brass block by the straps and the whole device was supported on three ⅛-inch ball bearings resting upon a $\frac{1}{16}$-inch brass plate.

Deformeter measurements made with only the crown gauge on the model were later checked after all the gauges and clamps were in place, thus showing that the presence of additional gauges and the method of clamping had not altered appreciably the original shape or elastic properties of the model.

In attaching gauges to the model an interesting problem arose which, fortunately, had been foreseen, namely, that the plug holes in some of the gauges were covered over by the model, thus making it impossible to insert the plugs from the top, as is usually done. The purchase of special gauges with the plug holes offset so as to clear the model was at first considered, but this would have involved much loss of time and additional expense. It was finally suggested that holes be bored in the drawing board directly under the plug holes in the gauges so that the plugs could be inserted from below. Three-quarter inch holes were made in the board where necessary before placing the model and subsequently the plugs were inserted through these with a pair of bent crucible tongs without difficulty.

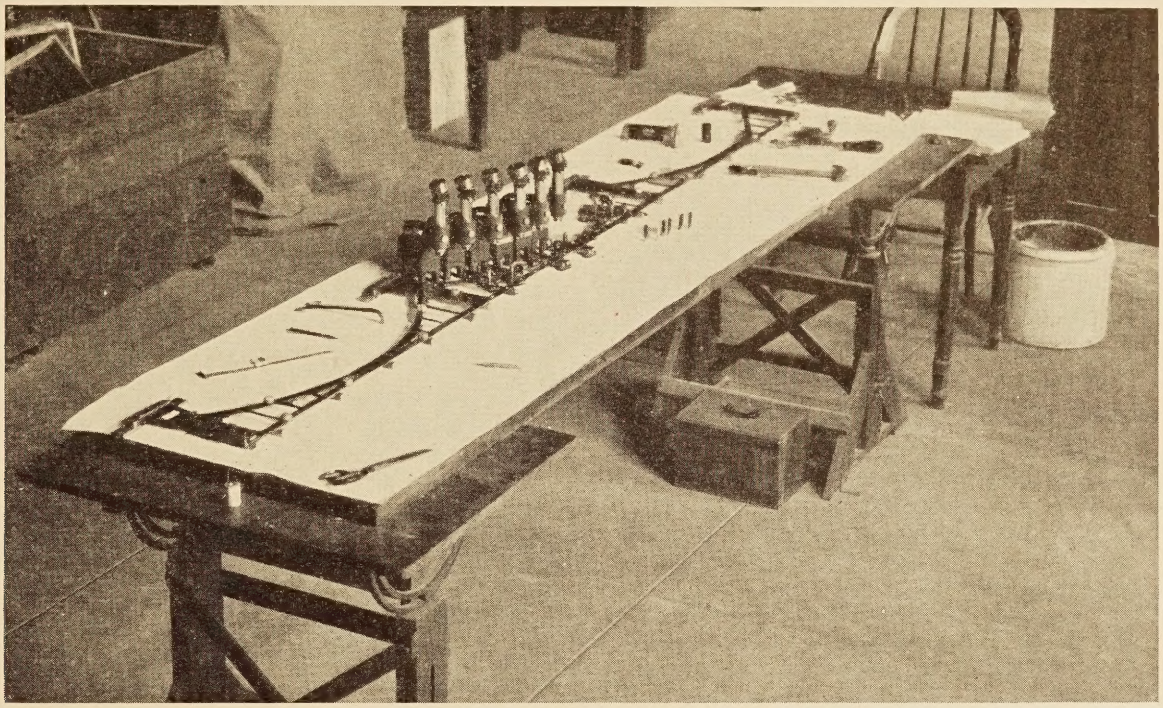

General View of Model and Apparatus

SIMPLE TECHNIQUE EMPLOYED

The work of making and recording the thousands of microscope readings was done by two men, one of whom manipulated the gauge plugs and read the microscope and the other recorded the readings.

The technique employed was very simple. Six microscopes were oriented and focussed upon six of the main targets, the proper plugs were inserted in the gauge under consideration, the temperature recorded, and the microscopes were quickly set upon the target points and read. The plugs were then changed, temperature was again recorded, microscopes were reset, and the second readings were taken. This was done as quickly as feasible, to permit as little temperature change as possible. The effect of temperature will be discussed later.

As soon as the thrust, shear, and moment data had been determined for the gauge and the microscope positions concerned the microscopes were shifted to six targets on the other half of the arch and the process was repeated for the same gauge. The difference between the two microscope readings for each point was then multiplied by the calibration coefficient of the microscopes and the thrust, shear, and moment influence diagrams for the point in question were plotted. In many cases, however, it was impossible to determine the true shape of the influence diagrams with readings from 12 positions of the microscopes and additional points usually had to be investigated. These additional points were selected so as to determine accurately the influence curve at points of sudden change of curvature.

To avoid errors in the sign of the microscope readings, a rule must be adopted and carefully followed if confusion is to be avoided. In the analysis under discussion the micrometer screws of the microscopes were always oriented in the same direction. The microscopes are so constructed that the orientation of the micrometer screw is independent of the microscope stand. This constant orientation, coupled with a definite order of plug insertion, practically eliminated this possibility of of error.

DIFFICULTIES SOLVED IN MAKING ANALYSIS

It was discovered at the beginning of the analysis that the two pairs of thrust plugs ordinarily supplied with the deformeter apparatus differed in diameter by so great an amount as to be unsuited for use with the model to be used. The model was so stiff that when the attempt was made to force the gauge bars far enough apart to insert the large thrust plugs the model was seriously distorted out of its normal plane. Conversely, when the small-size thrust plugs were inserted the gauge bars failed to close up snugly on the plugs. This effect was greatest between columns 3 and 3′, where the model offered great resistance to displacement of the sides of cut sections due to the stiffness of the very short columns and widened rib section, enlarged to represent the curtain wall. This difficulty was overcome by obtaining two pairs of thrust plugs which differed in diameter by a much smaller amount than the plugs regularly supplied. The difference in diameter of the plugs ordinarily supplied is 0.03599 inch; that of those used was 0.00539 inch.

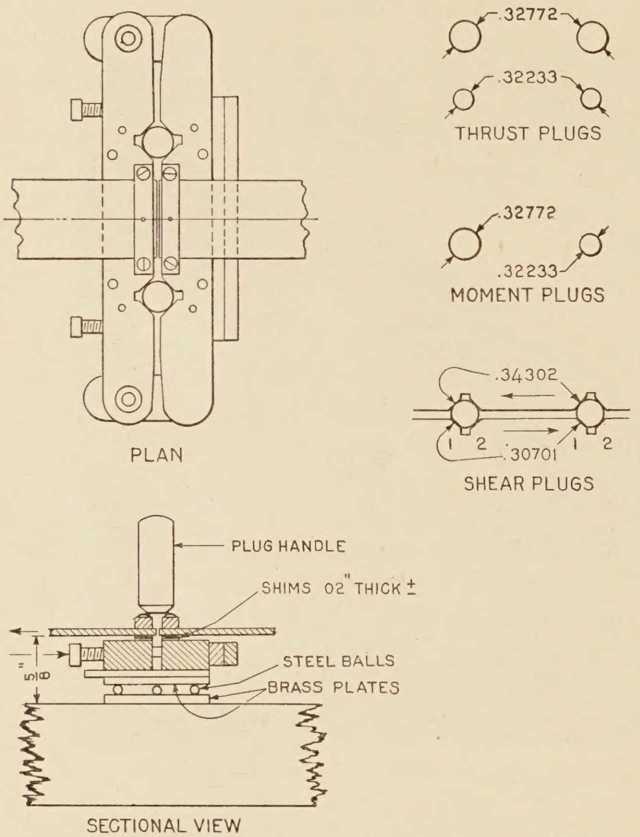

Fig. 2.—Beggs Deformeter Gauge

The stiffness of the model was responsible for another difficulty. The two bars of the gauge, are of course, supposed always to lie in the same plane so that the sides of the V-notches will be parallel and thus insure a snug fit against the plugs throughout the entire depth of the notches. It was noticed that in a few of the stiffer sections of the model the force exerted by the model upon the gauge bars, acting eccentrically with that of the springs holding the bars, produced an opposite rotation of the two bars about horizontal axes so that they no longer lay in the same plane. These forces are indicated by arrows in the sectional view of Figure 2. This condition was overcome by using a small C-clamp at each end of the gauge to draw the bars into the proper position.

The model was quite sensitive to temperature variations. This made it necessary to maintain as nearly as possible an even temperature in the room where the analysis was conducted and to manipulate plugs and read miscroscopes as quickly as practicable so as to reduce the temperature change in the interval between microscope readings to a minimum. All determinations involving temperature changes greater than 0.10° C. were thrown out. There were but few of these, however, due to the close temperature control effected by keeping the doors and windows of the laboratory closed. It was found that a puff of warm air coming through an open window would often send the temperature up a half degree centigrade in five minutes. Since it was not possible to work fast enough to keep the time interval between readings much below five minutes, and frequently longer, this was an important item.

Figure 3 shows a typical influence diagram for bending moment at the crown of the arch and how it is affected by a temperature variation of 0.5° C. It will be noticed that the percentage error is great only in regions of small microscope readings and that it is not large enough to be particularly serious at points of large readings. In the instance cited the percentage of error ranges from 100 per cent or more for the small readings to 8 per cent for the maximum reading at the crown.

Ordinarily the temperature variation will not be as great as 0.5° C. if precautions are taken, and most analyses are for the purpose of determining stresses where one is largely if not exclusively concerned with the large readings. In the present case, as will be seen later, small readings played a very considerable part in determining rotations which, unlike stresses, depend not merely upon the moment at the point where the stress occurs but upon the entire bending-moment diagram of the arch rib.

DEFORMETER DATA PRESENTED

A part of the deformeter data selected as typical is presented in the form of influence diagrams, Figures 4 to 17, inclusive. All of these pertain to the left half of the span, but those relating to similarly situated sections in the right half of the span display the expected symmetry. This form of presentation makes it possible to observe the many peculiar characteristics of the influence diagrams of analyses A and B (meaning of symbols explained below) in contrast with those of C, which follow very closely the theoretical influence diagrams of the free rib.

Some explanation of the meaning of the symbols A, B, and C seems necessary. The floor of the Yadkin River Bridge was of the conventional deck-girder type, with the ends of the girders resting upon spandrel columns without definite connection, the load being transferred to the supporting elements through a sole plate and a masonry plate. These plates were badly rusted together and thereby offered a large if not perfect resistance to displacements of a shearing nature. They were not, however, able to resist separation by direct tension or tension due to bending. As a matter of fact, it was observed that under certain loadings some of these plates actually separated on the tension side. The bending moments in the spandrel columns were dependent not only on the position of the load but upon the exact degree of fixity of the tops of the columns. The problem of accurately representing this condition in the model was one which had to be solved by the exercise of judgment rather than by accurate computations.

It was decided to make the first set of determinations upon a model cut out of solid material as if the girders had been built intergally with the columns. The con-

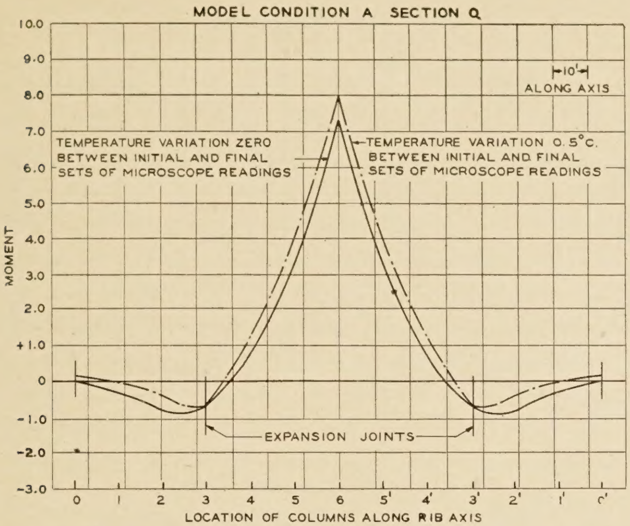

Fig. 3.—Typical Influence Diagram for Bending Moment at Crown and how it is Affected by Temperature Variation of 0.5° C.

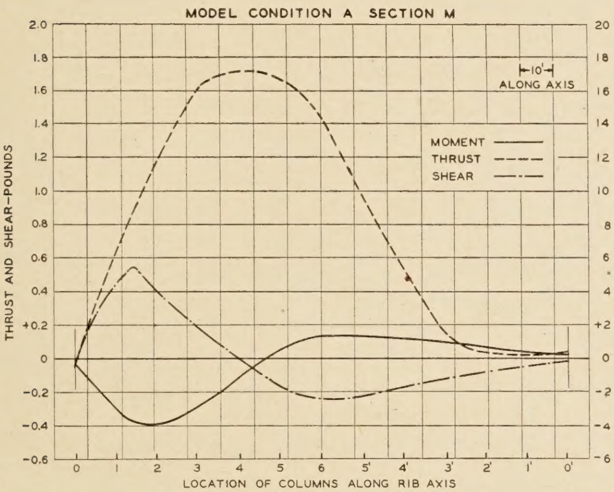

Fig. 4.—Typical Influence Diagram

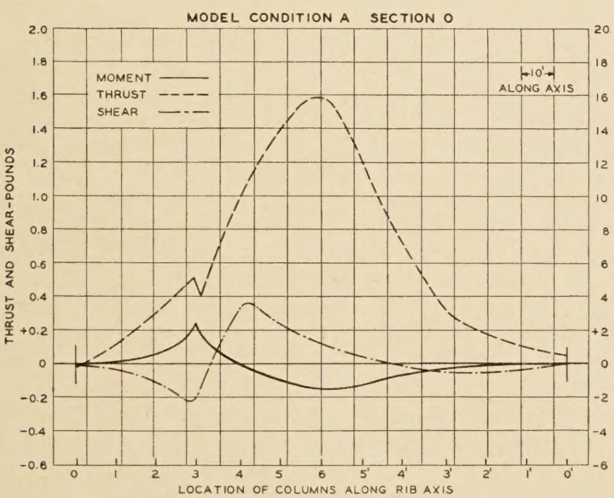

Fig. 5.—Typical Influence Diagram

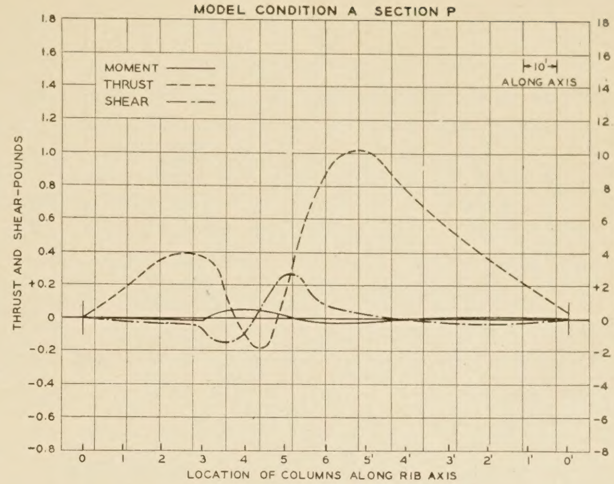

Fig. 6.—Typical Influence Diagram

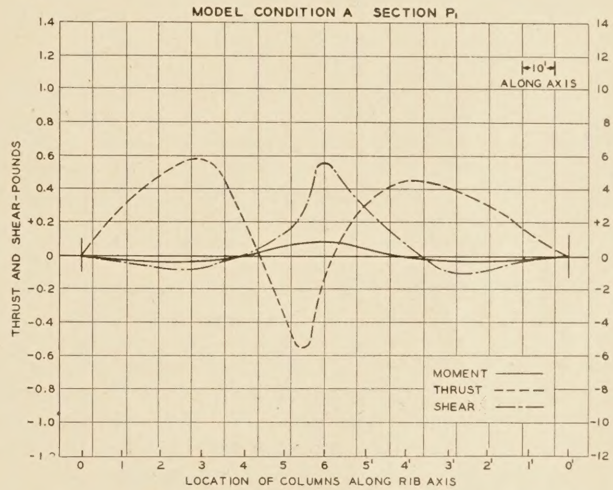

Fig. 7.—Typical Influence Diagram

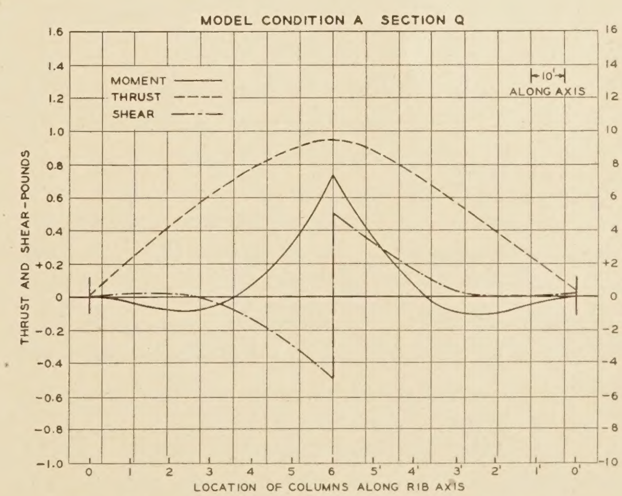

Fig. 8.—Typical Influence Diagram

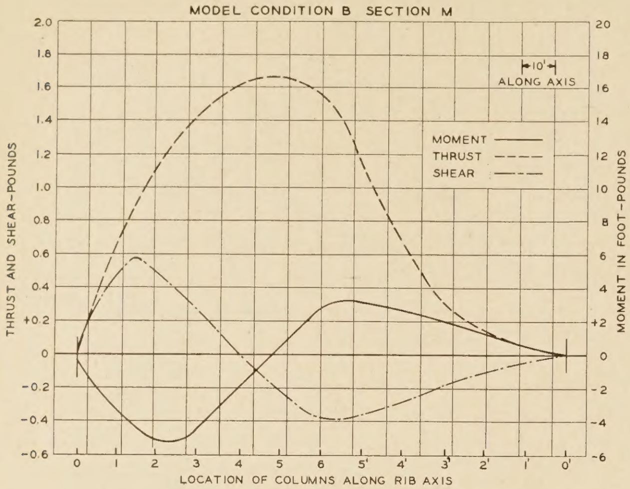

FIG. 9.—TYPICAL INFLUENCE DIAGRAM

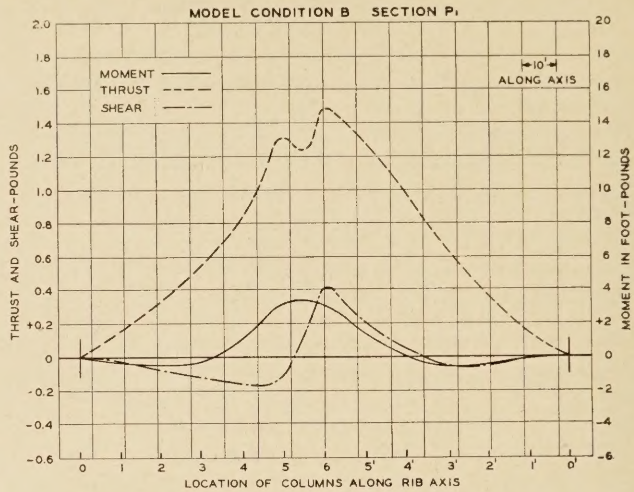

FIG. 12.—TYPICAL INFLUENCE DIAGRAM

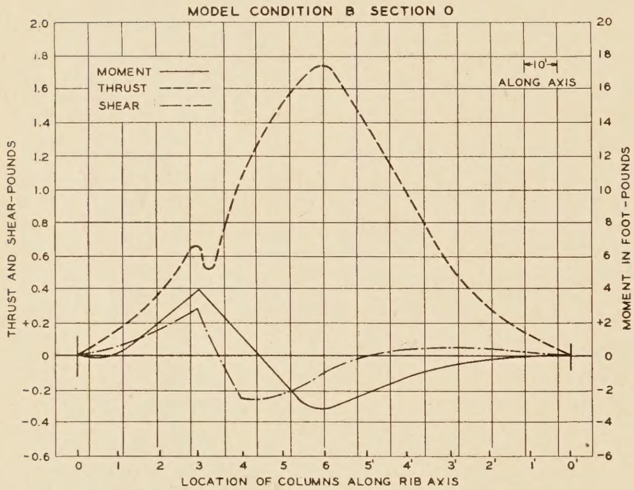

FIG. 10.—TYPICAL INFLUENCE DIAGRAM

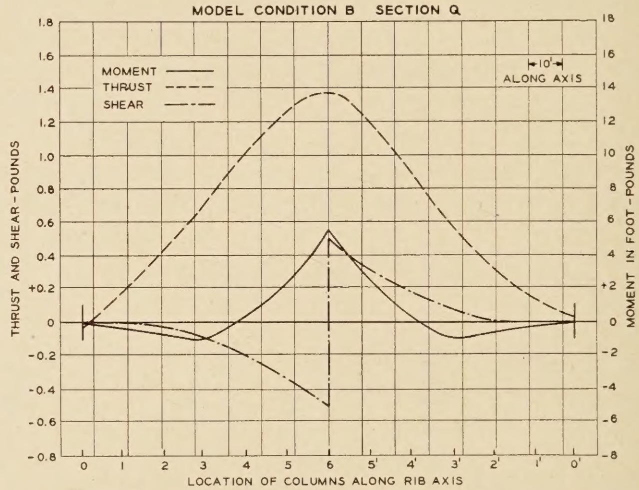

FIG. 13.—TYPICAL INFLUENCE DIAGRAM

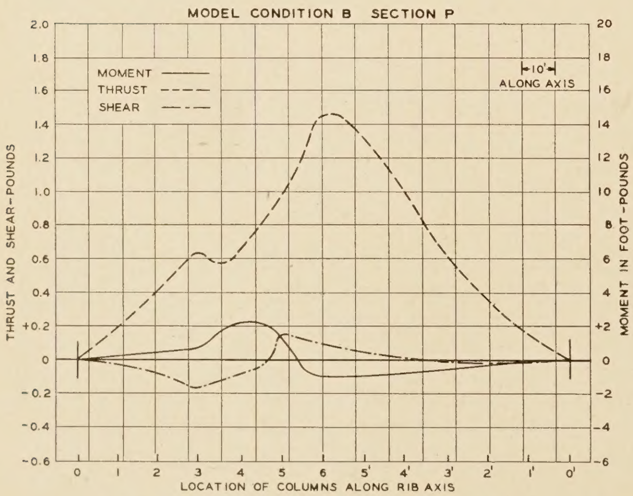

FIG. 11.—TYPICAL INFLUENCE DIAGRAM

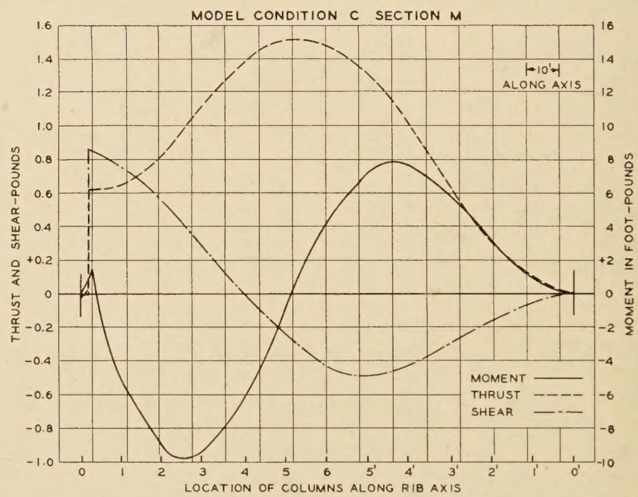

FIG. 14.—TYPICAL INFLUENCE DIAGRAM

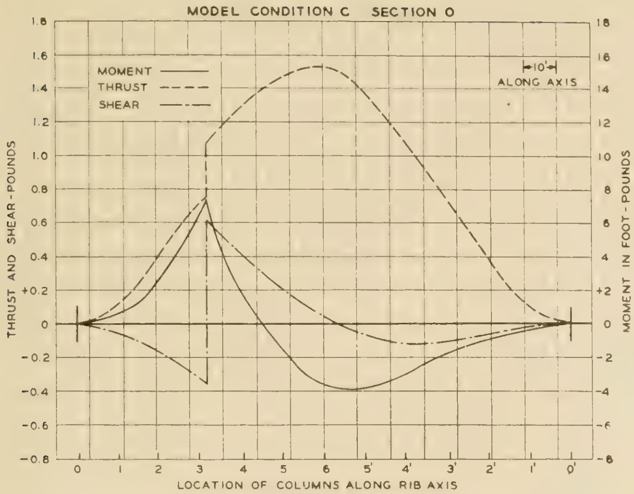

FIG. 15.—TYPICAL INFLUENCE DIAGRAM

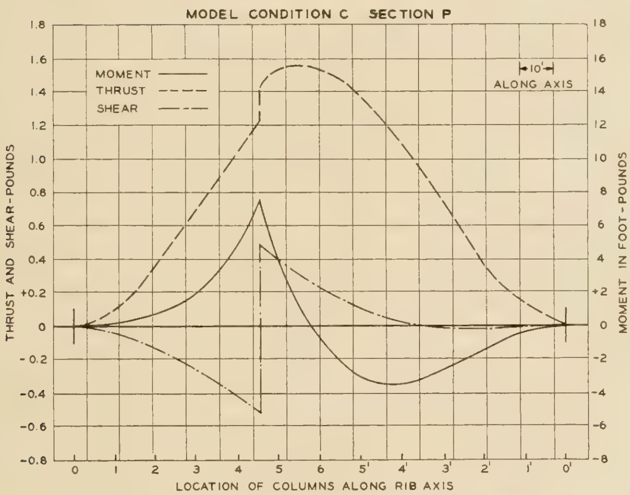

FIG. 16.—TYPICAL INFLUENCE DIAGRAM

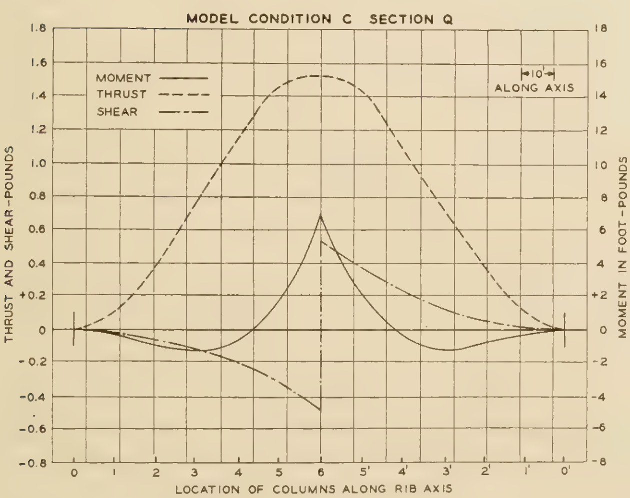

FIG. 17.—TYPICAL INFLUENCE DIAGRAM

nections of the girders and columns were then modified in an attempt to bring about a simulation of the conditions described for the actual structure. Later the entire floor and spandrel construction was cut loose, leaving only the free rib, this condition corresponding to a series of measurements made upon the Yadkin River Bridge after the continuity of the deck had been completely destroyed.

The modification of the girder connections was effected by severing the tops of the columns from the underside of the floor and welding on a small celluloid link with a drop of acetone. The construction of the links and the manner of connecting them is shown in Figure 18.

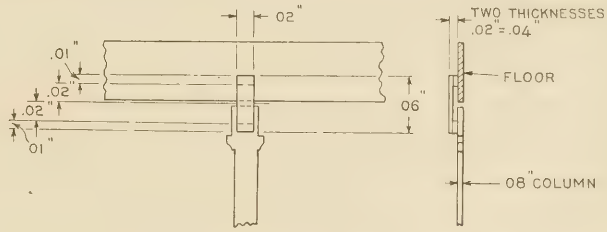

FIG. 18.—DETAILS OF CONNECTING LINK

The three conditions of test resulting from the foregoing were designated as follows: Floor and columns integral, with microscope readings taken on the floor, condition A; column connections modified, with readings on the floor, condition B; floor, spandrel construction and curtain wall removed, with readings on the free rib, condition C.

INFLUENCE DIAGRAMS USED IN COMPUTING STRESSES AND ROTATIONS

The influence diagrams, Figures 4 to 17, were used in computing the extrados and intrados stresses shown in Figures 4 to 13 of the main report[4] (typical graphs shown on p. 218) which also show measured stresses and theoretical stresses computed for the free rib. The two ordinates corresponding to the two points of application of test load (68,250 pounds) were picked from the thrust influence diagram for the particular section involved. These ordinates were then added and multiplied by 68,250, the result being the total thrust applied to the section. The bending moment at the section was obtained from the moment influence diagrams in a similar manner. The extrados and intrados stresses were then computed from the were known formula

$$f = \frac{P}{A} \pm \frac{My}{I} \text{ in which}$$

f = unit fiber stress in concrete,
P = total direct stress,
A = combined area of section (steel and concrete),
M = bending moment at section,
y = distance from neutral axis to extreme fiber,
I = combined moment of inertia (steel and concrete) of section.

In computing the values of arch rib rotation shown in Figures 27 and 28 of the main report, which also show the measured values and the theoretical values computed for the free rib, it was first necessary to

[4] Public Roads, vol. 9, No. 10, December, 1928.

make bending-moment diagrams for the entire arch rib for each of the three conditions of model analysis and five positions of load. A typical bending-moment diagram, for a load of unity, is shown in Figure 20. One value of bending moment was measured directly by deformeter gauges in each panel (usually about midway between columns), while the values shown at each side of the columns and at the springing points were computed from the thrust, shear, and moment at the adjacent gauges.

The construction of a diagram showing the variation of EI for the rib was also necessary before the rotations, $\Sigma \frac{Mds}{EI}$ could be computed. This diagram is shown in Figure 19 in which the sudden increase in values at columns 3 and 3′ is due to the presence of a curtain wall which was constructed integrally with the rib of the structure between these columns.

The diagram for values of EI was plotted upon tracing cloth and when this was superimposed upon the bending-moment diagrams it was possible to pick directly from the combined diagrams the bending-moment ordinates M, the length of the rib segment ds, and the corresponding value of EI. Values of $\frac{Mds}{EI}$ were so obtained for each successive length of rib beginning at the springing point and tabulated. In order to determine the rotation at any given section it was only necessary to sum up, algebraically, the tabulated values between the springing point and the section in question.

The algebraic summation of these values of $\frac{Mds}{EI}$ taken from end to end of the rib should, of course, equal zero. Actually the values when added failed to balance, the discrepancy amounting to as much as 16 per cent in the case of analyses A and B. However, for analysis C the balance was very close. In each case the error was distributed before computing the rotations.

MODEL RESULTS COMPARED WITH THEORETICAL AND ACTUAL STRESSES

Figures 4 to 6 of the main report (see p. 218) show the theoretical values of stresses computed for the free rib and the stresses measured on the actual structure with the deck intact. The lines connecting plotted points are not intended to indicate variations in stress between points but merely as a guide for the eye. In these diagrams the model analysis results have also been shown for condition A, floor and spandrel construction integral, and condition B, floor and spandrel columns connected with links.

The model stresses show a general correspondence with the measured ones, the results of analysis B being particularly close to the measured stresses. This indicates that the method adopted to make the model of analysis B fit the structure was a fair approximation. The stresses of analysis A are in practically every case lower than either those of analysis B or the measured ones, which is to be expected because of the stiffer condition of the model.

As pointed out in the main report, a comparison of the theoretical rib stresses with either the measured stresses or those derived from the model strikingly reveals the reduction in rib stresses due to the stiffening effect of the superstructure and curtain wall. Taking this effect into consideration makes possible material economies in the design of such a rib. The question which naturally arises as to the applicability of the deformeter method to such a design is discussed later.

Figures 10 to 13 of the main report (see p. 219) show the theoretical stresses computed for the free rib and

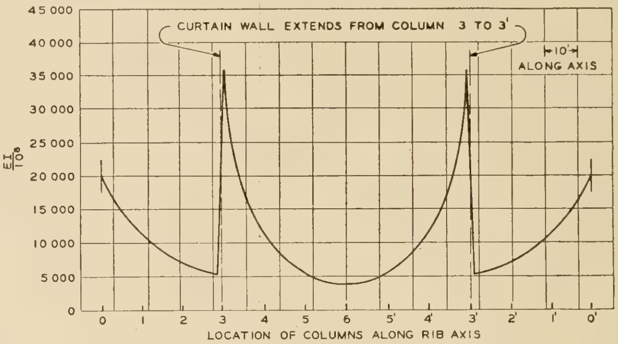

Fig. 19.—Diagram Showing Variation in EI

the stresses measured with the continuity of the deck destroyed so that the test loads were applied directly to the arch rib by means of the spandrel columns. These diagrams also show the stresses resulting from model analysis C, with the superstructure and curtain wall removed from the model rib. No measurements were made with loads at columns 1 and 2 because of danger involved in such loading; consequently no curves are submitted for this condition. A crack developed in the concrete of the intrados between the gauge points of the crown telemeter and measured stresses are therefore not shown for this point.

A study of these curves reveals that the theoretical stresses and the model stresses check almost exactly. This is of particular interest in view of the fact pointed out in the main report that, all things considered, the curves of measured stresses also check the theoretical curves very well. They show the same general variations and in at least 75 per cent of the cases plotted the results are remarkably close.

These curves should go a long way toward allaying any doubt that may exist as to the applicability of the elastic theory to the design of free arch ribs. Here we see the stresses predicted by the theory essentially substantiated in the reinforced concrete structure and further substantiated in a homogeneous elastic model of the structure.

BENDING MOMENT DIAGRAM INDICATES STIFFENING EFFECT OF SUPERSTRUCTURE

A typical bending-moment diagram of the arch rib for the three conditions of model analysis is shown in Figure 20. The effect of the superstructure is clearly indicated by comparing the theoretical bending-moment diagram, computed for the free rib with those resulting from model analyses A and B. The results of analysis C correspond closely to the theoretical.

The great difference between moments existing on either side of the columns of model analyses A and B represents the bending moments carried by the columns at their lower ends and introduced by them into the rib. The reader is likely to wonder what happens to the columns under these moments and to think that economies effected by taking the superstructure into

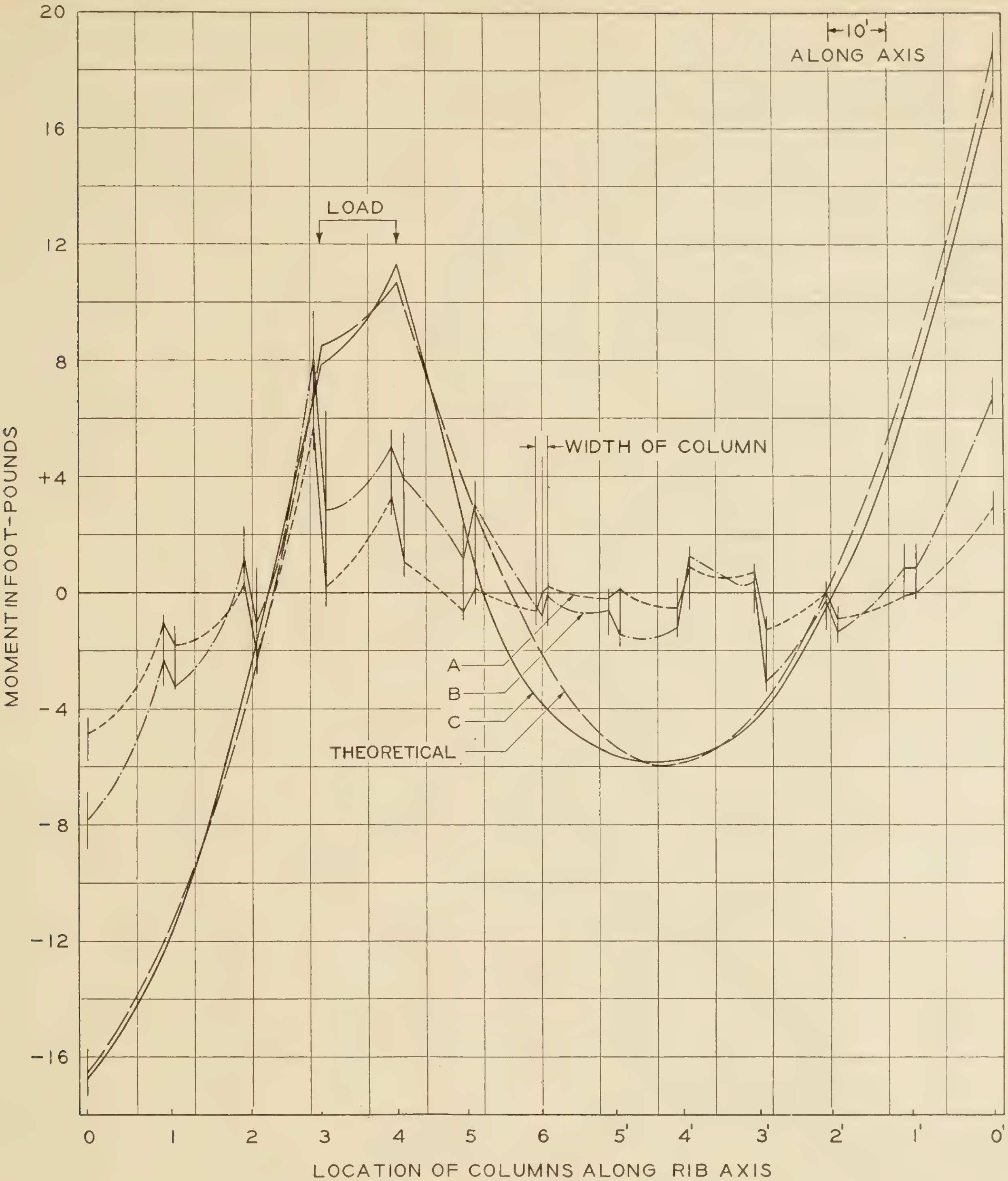

Fig. 20.—Typical Bending-Moment Diagrams for Unit Loads

consideration in designing would be largely offset by the additional material necessary to make the columns strong enough to resist these high moments. As a matter of fact, the columns between 3 and 3′, inclusive, existed only in the model; the actual structure, following common practice, had a curtain wall between these columns.

In order to throw some light upon what stresses might be expected in spandrel columns, the two most heavily stressed ones were investigated, i. e., column No. 2, existing in both the structure and the model and column No. 4, existing in the model only. In both cases maximum stress conditions were found with loads placed at columns Nos. 2 and 3. For the test load of 68,250 pounds, without impact, the maximum fiber stresses, including dead load, were found to be 880 pounds per square inch compression and 430 pounds per square inch tension for column No. 2, whereas for column No. 4 these amounted to 1,870 and 1,630 pounds per square inch, respectively. For the commonly specified 20-ton truck, or 125 pounds per square foot of floor, both with 30 per cent impact, the maximum fiber stresses, including dead load, were found to be 305 pounds per square inch compression and 75 pounds per square inch tension for column No. 2, while for column No. 4 these amounted to 580 and 460 pounds per square inch, respectively.

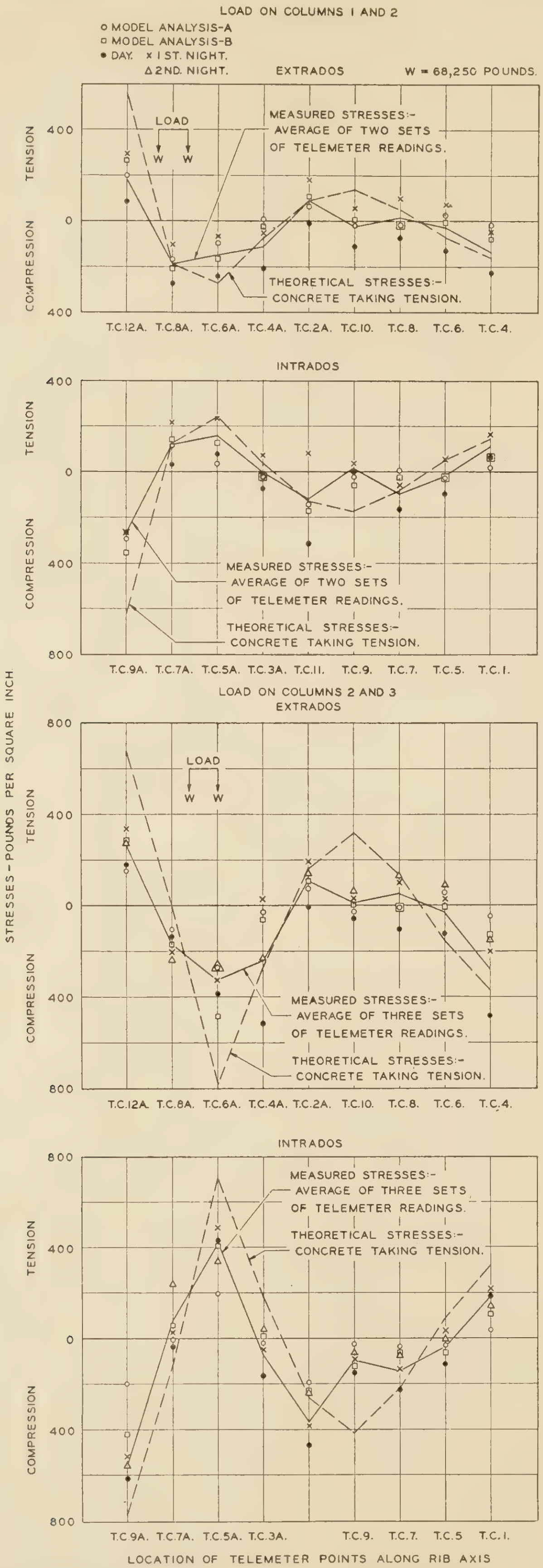

FIGURE 4 OF MAIN REPORT SHOWING STRESSES IN ARCH RIB UNDER 1-TANK LOADING WITH DECK INTACT

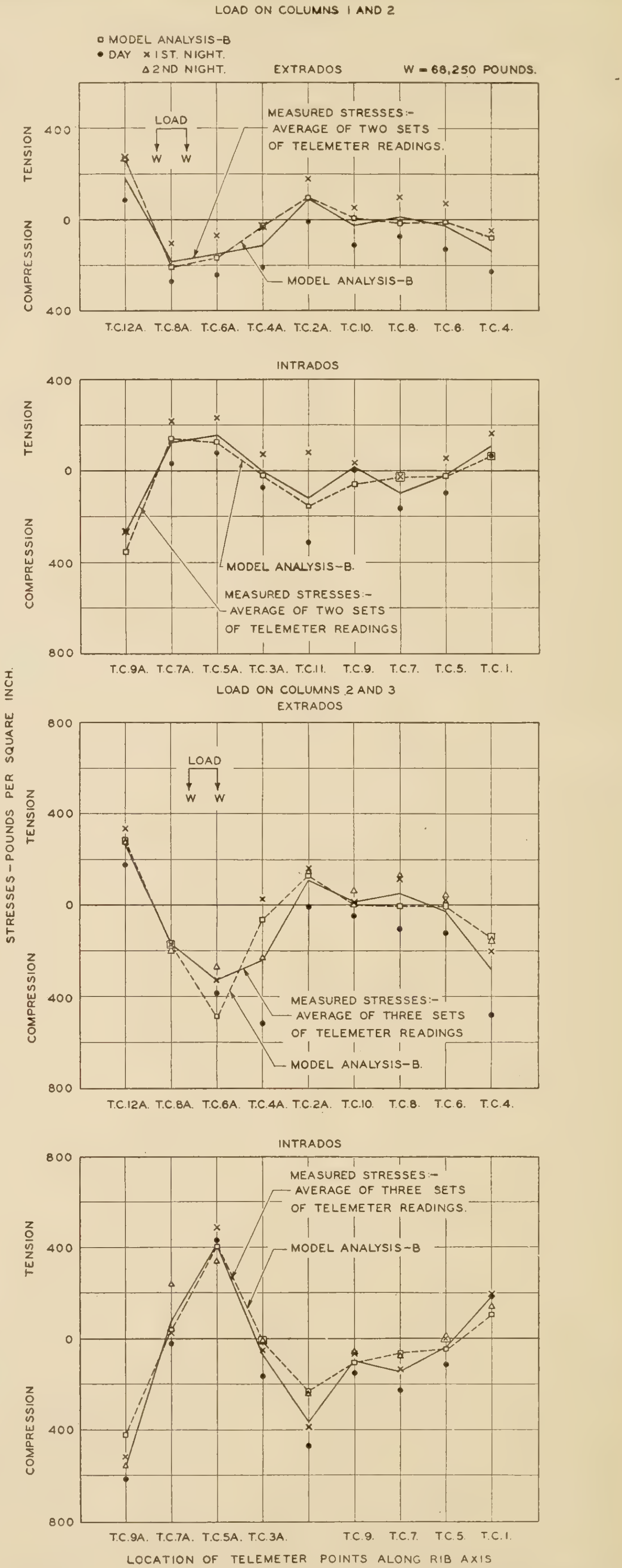

FIGURE 7 OF MAIN REPORT, SHOWING COMPARISON OF MEASURED STRESSES IN ARCH RIB UNDER 1-TANK LOADING WITH DECK INTACT AND MODEL ANALYSIS B

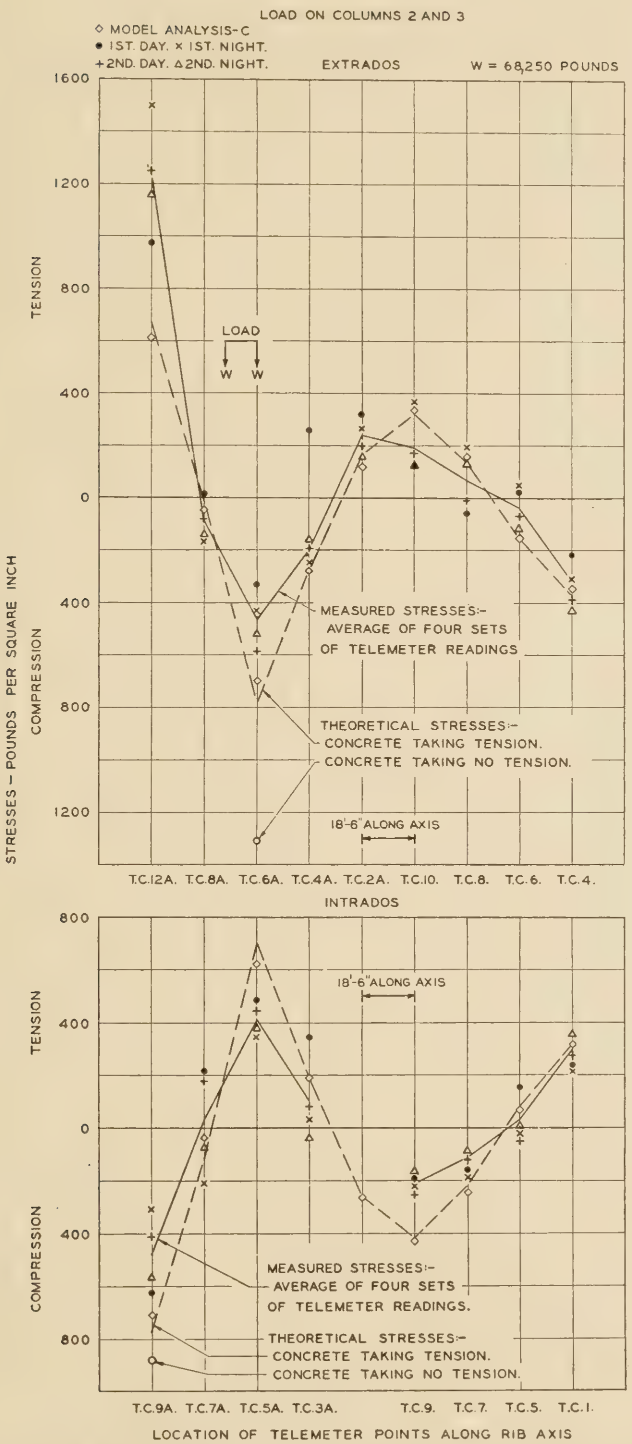

FIGURE 10 OF MAIN REPORT, SHOWING STRESSES IN ARCH RIB UNDER 1-TANK LOADING WITH DECK CUT

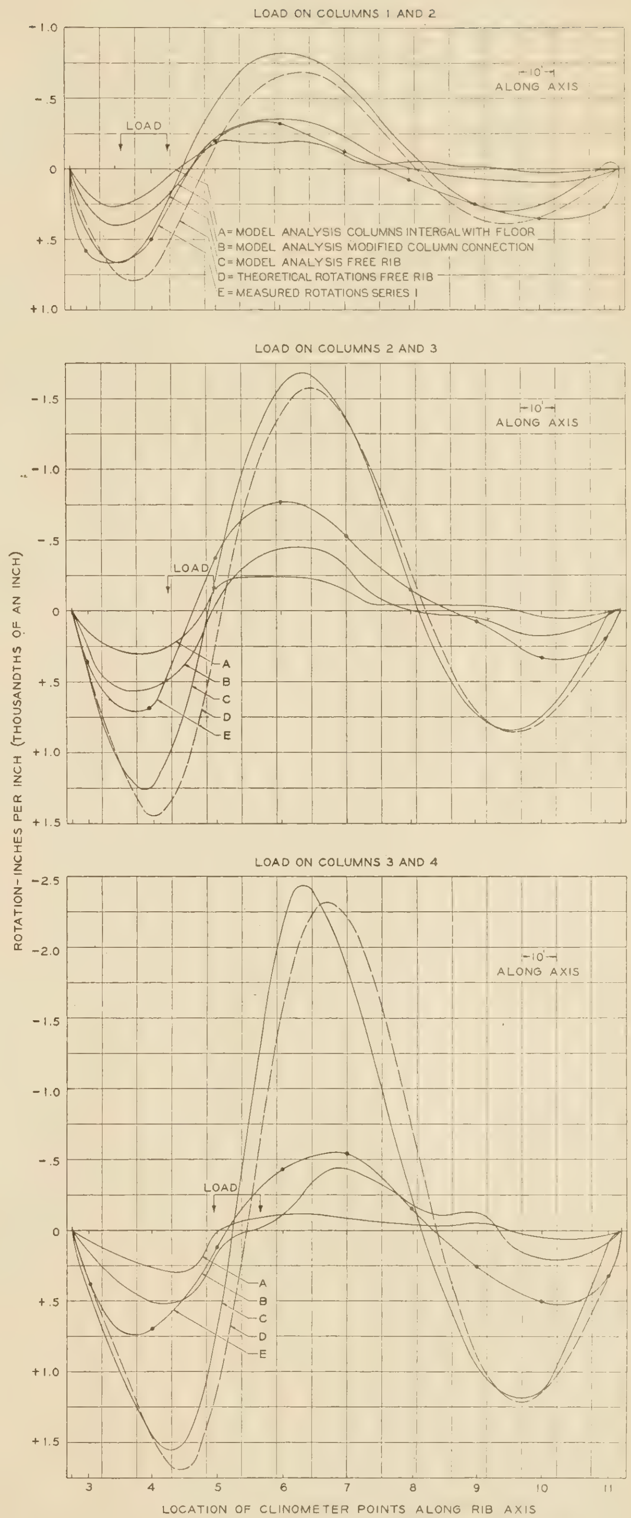

FIGURE 27 OF MAIN REPORT, SHOWING ROTATIONS OF ARCH RIB UNDER 1-TANK LOADING FROM MODEL ANALYSIS COMPARED WITH MEASURED ROTATIONS

MODEL RESULTS COMPARED WITH THEORETICAL AND ACTUAL ROTATIONS

Curves A, B, and C of Figures 27 and 28 of the main report (see p. 219) show the results of analyses for the three model conditions. Curve D shows the theoretical rotations computed for the free rib and curve E shows the rotations measured with the deck intact. Rotations measured with the continuity of the deck destroyed are omitted in order to avoid confusion. These values, however, check the theoretical values at least as closely as do the values of model analysis C. The fact that curves C and D check the measured rotations with the deck cut is further evidence of the applicability of the elastic theory to the design of free arch ribs.

The measured results and the model results A and B are consistently less than the theoretical results, again indicating the stiffening effect of the superstructure with its attendant possibilities of economy.

The rotations of analysis B with the floor-beam connections of the model replaced with celluloid "links" are consistently closer to the measured results than are those of analysis A for the unmodified floor condition. In the discussion of the stress curves it is argued that because the stresses of model analysis B check the stresses measured with the deck intact the method of modifying the floor-beam connections of the model was successful. In the rotation curves under consideration the model rotations B when compared with the rotations E, measured with deck intact, bear out this fact, although it is not at first apparent. This is because the individual values do not check. However, the slopes are largely very similar, and it is the slopes of the curves which are important. This is true because the slope is directly proportional to the bending moment divided by the moment of inertia of the section, and, therefore, at any particular point on the arch axis where the curve slopes are the same the bending moments are the same. Since rib stress is very largely due to moment, the rotation curves as well as the stress curves indicate that the model with the floor modified corresponded fairly closely to the actual structure with the deck intact.

BEGGS METHOD ADAPTED TO CHECKING COMPLICATED DESIGNS WHERE DEFINITE CONNECTIONS ARE USED

For simple structures such as a free arch rib the Beggs method possesses a very high degree of accuracy. It is easily possible to read microscope settings to a half of a scale division of the micrometer head, which means, for the plugs and calibration factors used in this analysis, an accuracy of 0.05 foot-pound for moment, 0.01 pound for thrust, and 0.002 pound for shear when the influence load is 1 pound. The calibration factors by which microscope readings were multiplied in order to reduce them to influence diagram ordinates are $\frac{5}{53.07}$, $\frac{1}{39.74}$, and $\frac{1}{264}$ for moment, thrust, and shear, respectively.

For complicated structures the accuracy is somewhat reduced. It was noticeably more difficult to obtain check readings on individual influence diagram ordinates of the A and B analyses than for the free rib condition C.

The effect of temperature is serious, particularly in the case of complicated structures where microscope readings are more likely to be small and where oftentimes plugs of smaller diameter differences must be employed. The degree of accuracy which can be obtained with the Beggs apparatus will certainly be enhanced by controlling temperature variations to a greater degree than is commonly met with in the average drawing room.

The problem of truly representing a given structure by a model is of outstanding importance. Such features of construction as curtain walls, which are an integral part of the structure, can be represented with considerable accuracy. In representing the conditions of indefinite connections such as were met with in the case of the expansion joints and the bearing-plate contact between the deck and spandrel construction of the Yadkin River Bridge, it must be admitted that any modification of rigid connections in the model is little better than an estimate.

Because of this difficulty, which definitely reduces the Beggs method to the realm of uncertainty and which is accentuated by the fact that the effect of any attempt to represent indefinite connections varies with the position of load as well as other factors, it is felt that where this method is contemplated in design it will be well to consider using definite connections in the structure. Where this is done there appears no serious reason why the method is not well adapted to checking designs of a complicated nature.

CONCLUSIONS

1. The behavior of the free rib as calculated by the elastic theory is in close agreement with that determined by the model analysis.
2. The model analysis shows that the presence of the superstructure acts to reduce rib stresses.
3. In model analyses similar to that made of the Yadkin River Bridge considerable care must be exercised to maintain a fairly uniform room temperature during operations.
4. It is indicated by the relatively greater difficulty encountered in securing check results that the accuracy of the Beggs method is somewhat decreased as structures grow more complicated.
5. Where the application of the Beggs method to design is contemplated provision should be made for definite connections in the structure. Otherwise the problem of representing the structure by a model becomes very uncertain.

MOTION PICTURE OF YADKIN RIVER BRIDGE TESTS AVAILABLE

A motion picture showing details of the Yadkin River Bridge tests, reported in this and the preceding issue of PUBLIC ROADS is now ready for distribution. The picture has been prepared by the Office of Motion Pictures of the United States Department of Agriculture for the Bureau of Public Roads.

The picture shows the method of loading, test apparatus in place, measurements being taken, and closes with scenes taken during the destruction of the bridge with explosive in experiments by the War Department.

About 20 minutes are required for showing the film, which is available for use on specific dates upon the condition that the borrower pay the cost of transportation. Requests for the film should be directed to the Office of Motion Pictures, United States Department of Agriculture, Washington, D. C.

INFLUENCE OF MINERAL COMPOSITION OF SAND ON MORTAR STRENGTH

Reported by E. C. E. LORD, Petrographer, Division of Tests, United States Bureau of Public Roads

Tests recently completed by the Bureau of Public Roads on 100 samples of sands from Maine have given some indication of the effect of certain mineral constituents on the strength of mortar. It should be stated, however, that the materials examined were obtained from a relatively limited area and that any deductions drawn from the test results may not necessarily be applicable to sands of similar composition but deposited under widely different conditions.

While the Maine sands vary greatly in composition, as previously reported by Leavitt and Gowen,[1] 67 of the samples were found to contain orthoclase feldspar and quartz as essential constituents associated with small quantities of mica and occasionally fragments of granite and granitic gneiss. In some cases small quantities of sandstone and schist were also identified. On the whole, these 67 sands are distinctly of granitic origin and differ from the remaining varieties in the angularity of grain, indicative of very short transportation from source of origin.

The remaining sands, comprising 33 samples, were composed essentially of rounded fragments of quartz, sandstone, and slate, with varying quantities of shale, schist, and limestone, and were derived chiefly from sedimentary or metamorphic rock formations.

The angular constituents of the granitic sands might lead to the assumption that they would yield greater mortar strength than the more rounded sands from sedimentary rocks, but in regard to tension, at least, this was found not to be the case. (See report by Leavitt and Gowen.[1]) The results of the laboratory tests should not, however, be taken as conclusive evidence of the superiority of the sedimentary sands over those derived from granitic rocks, as the constituents of the former, especially shale and slate, may well be less resistant to disintegration under severe atmospheric conditions than the quartz and feldspar of the granitic sands.

Table 1 gives the results of the tests for both types of sand. The test specimens (briquets and 2 by 4 inch cylinders) were made of 1:3 mortar of normal consistency and tested at 7 and 28 days. Tests were also made on Ottawa sand mortar in order to determine the strength ratio.

Only the results of strength tests with sands having 20 per cent or more retained on a No. 14 sieve have been tabulated. Eighty-three of the sands met this requirement, while 13 were found to contain so much clay and silt as to be unsuitable for an analysis of this character. In Table 1 the 83 sands have been divided into the two major groups according to origin. Each group has also been further subdivided according to the amount retained on the No. 14 sieve to bring out relations which may exist between the strength ratio and the grading of the sand. These values have all been plotted in Figure 1, which brings out the interrelationships existing between mineral composition, strength, and grading in a very interesting manner.

[1] Mineral Content of Maine Sands in Relation to Mortar Strength, by H. Walter Leavitt and John W. Gowen, Proc. Nat. Acad. Sciences, vol. 13, No. 6, June, 1927.

Comparing the average tensile strength ratio for groups A and B at 7 and 28 days (fig. 1), we find that the average ratio for the feldspathic group is only 73 per cent of the corresponding values for the nonfeldspathic group at 7 days and only 66 per cent of the nonfeldspathic group at 28 days. In compression both sand types yield mortars having about equal strengths at both testing periods.

The tests show a decrease in tensile strength ratio at 28 days compared with that for the 7-day period for mortars containing both types of sand. In compression, however, practically the same strength ratio is noted for both periods.

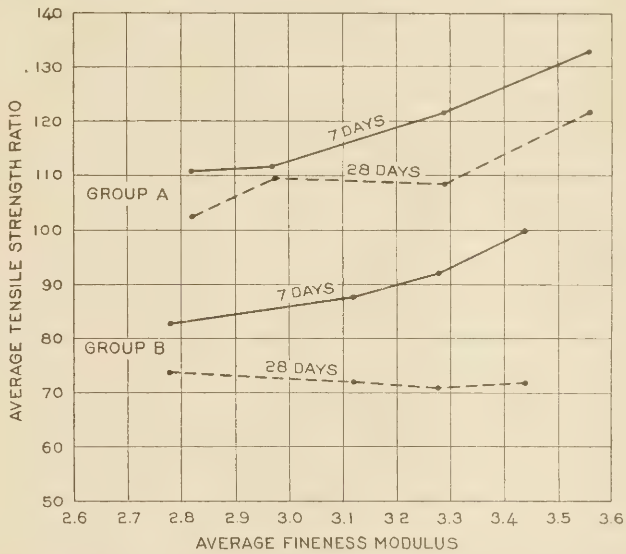

Fig. 1.—Relation Between Grading, Mineral Composition, and Strength of Concrete Sands. Group A Composed Essentially of Quartz, Sandstone, and Slate. Group B Composed Essentially of Quartz, Feldspar, and Mica.

Table 1.—*Results of tests*

GROUP A.—SANDS CONSISTING ESSENTIALLY OF QUARTZ, SANDSTONE, AND SLATE

Number of samples tested	Average fineness modulus	Retained on No. 14 sieve	Tensile strength ratio		Compressive strength ratio	
			7 days	28 days	7 days	28 days
		Per cent				
7	3.56	50–60	133	122	120	128
5	3.29	40–50	122	109	116	102
11	2.97	30–40	112	110	107	105
6	2.82	20–30	111	103	103	102
Weighted average	3.14	20–60	119	111	111	109

GROUP B.—SANDS CONSISTING ESSENTIALLY OF QUARTZ, FELDSPAR, AND MICA

Number of samples tested	Average fineness modulus	Retained on No. 14 sieve	Tensile strength ratio, 7 days	Tensile strength ratio, 28 days	Compressive strength ratio, 7 days	Compressive strength ratio, 28 days
1	3.44	50–60	100	72	121	128
11	3.28	40–50	92	71	119	117
17	3.12	30–40	88	72	115	114
25	2.78	20–30	83	74	103	105
Weighted average	3.01	20–60	87	73	110	111

It is probable that the inherent weakness of mortar made with granitic sand of the types considered is due largely to the feldspar component, as the quartz is perfectly sound and the mica is present in quantities too small to appreciably affect the mortar strength. Comparing the appearance of granitic sand with freshly crushed granite screenings, it is observed that the flesh-colored tint usually apparent in the fresh granite is largely replaced by a grayish brown color, due to oxidation and hydration of iron compounds present in the granite. This coloration is an indication of weathering and is confined generally to the feldspar constituent of the sand. In some cases the weathering has advanced so far that kaolin-like products of decomposition occur which sensibly decolorize dilute aniline dye solutions. The natural cleavage of the feldspar, rendered more pronounced by weathering, causes the individual feldspar grains to part readily when subjected to tensile stresses, thereby lowering the strength of the mortar. That the tensile-strength ratio is lower at 28 days' than at 7 days' curing may be explained by presuming the early strength to be controlled largely by the strength of the cement binder, regardless of the quality of the aggregate, whereas, later on, as the cement increases in strength, the inherent weakness of the feldspar grains becomes effective in reducing the normal strength of the mortar. The weakness of the feldspathic grains at the 28-day period is apparently the controlling factor, entirely overshadowing the effect of grading which is indicated at 7 days.

Compression tests, however, indicate that the structural weakness of the feldspar is largely overcome by the angularity of the grains, which, when interlocked with angular quartz, produce mortar aggregates offering as great a resistance to shear as the grains of quartz, sandstone, and shale.

The results obtained from this investigation indicate that sands of the general character of those examined which contain an appreciable quantity of feldspar in a more or less weathered condition should be avoided in mortar or concrete subject to tensile stresses.

A PROPOSED ABRASION TEST FOR SAND INVESTIGATED

Reported by D. O. WOOLF, Assistant Materials Engineer, United States Bureau of Public Roads

SANDS PROPOSED for use in concrete are subjected to certain tests to determine their suitability and to predict as far as is possible their effect upon the quality of the resulting concrete. These tests include a mechanical analysis to determine the grading of the material, a chemical test to detect the presence of organic matter, a washing test to determine the amount of clay and silt present, and a strength test of the sand mortar. The strength test is usually a tension test on mortar briquets and the results are commonly expressed as the ratio between the strength of a mortar using the sand in question and that of a mortar of the same proportions and consistency using standard Ottawa sand. This tensile-strength test ratio in many cases has been considered to furnish, directly, an index of the concrete-making properties of the sand. The test, however, fails to accomplish this purpose.

It is known that the results of the tension test are not dependent on the quality of the sand alone, but are affected to a great degree by the grading of the sand, the amount of silt and clay, or the presence of organic or other impurities. These factors are inherent in the test; other factors such as the consistency of the mortar and the strength of the cement used, the method of molding, and temperature of the mixing and storage water, etc., may affect the results to a marked extent, but as these can be controlled they need not be considered further in this discussion.

None of the routine tests ordinarily made on concrete sands directly determine the quality of the sand grains. The present practice in concrete-road construction results in the coarse aggregate being worked away from the surface, and it is apparent that sands composed of hard and durable grains are advantageous in order that the mortar surface thus formed may resist the abrasive action of traffic. The object of the investigation described in this paper was to devise a simple laboratory test which would indicate the resistance to wear or abrasion of sand grains. It is believed that if a test can be devised which will indicate the quality of the sand grains alone it will be a great improvement over the present test.

PROPOSED ABRASION TESTS HAVE BEEN UNSATISFACTORY

In 1915 F. L. Roman, at that time testing engineer for the Illinois Highway Department, published a paper [1] describing an abrasion test for sand. The test consisted of removing from a sample of sand the material over ¼-inch and under the 50-mesh, and subjecting a given weight of the residue to the impact and abrasion produced by a certain number of small steel balls when run in the standard Deval abrasion machine. No effort was made to eliminate the effect of grading. The results were not very reliable and the test was not generally adopted.

In 1925 John W. Gowen and H. Walter Leavitt, of the University of Maine, published a paper [2] describing an abrasion test for sand which is an improvement over Roman's original test method. Gowen and Leavitt used a 500–gram sample of sand passing the 14-mesh and retained on the 28-mesh sieves, with an abrasive charge of eighteen ¾-inch steel balls and a test run of 2,000 revolutions in the Deval machine. The material passing the 100-mesh sieve after the test run was considered the loss by abrasion.

In the Roman test different samples of sand can not be compared as to their resistance to abrasion unless they have the same grading. The Maine method is open to the objection that only a portion of the entire sand sample is subjected to test. It has not been demonstrated that any one size of sand grain

[1] Wearing Tests for Sand and Gravel, Good Roads, vol. 9, p. 186, May 1, 1915.
[2] Bulletin No. 13, Maine Technology Experiment Station, A Method of Measuring Hardness and Durability of Sand.

is representative of the entire material, and for this reason it seems desirable to include a portion of each size in the sample as prepared for test. Table 1 gives the results of a series of tests on a local sand, each size being tested separately, as well as in two definite gradings. These results indicate that in order to obtain directly comparable results between different sands the grading must be controlled and the test sample should be representative of the major portion of the sand.

Table 1.—Results of abrasive tests on sands of different grading

Grading	Percentage of wear
¼-inch[1] to 10-mesh	2.8
10-mesh to 20-mesh	4.6
20-mesh to 30-mesh	5.8
30-mesh to 40-mesh	8.0
40-mesh to 50-mesh	14.3
Coarse grading (¼-inch to 50-mesh)[2]	9.4
Fine grading (¼-inch to 50-mesh)[2]	10.9

[1] The ¼-inch screen mentioned in this paper has round openings.
[2] The gradings used here are as follows:

Size	Percentage in test sample	
	Coarse	Fine
¼-inch to 10-mesh	30	20
10-mesh to 20-mesh	30	20
20-mesh to 30-mesh	20	25
30-mesh to 40-mesh	10	20
40-mesh to 50-mesh	10	15

SATISFACTORY RESULTS SECURED WITH NEW METHOD

To remove this effect of grading, two methods were proposed; first, to test all samples using a certain standard grading; second, to test the sample using its natural grading and to run accompanying tests on a standard sand with the same grading as the sand under test, expressing the results as the ratio between the percentages of wear of the two sands. It was decided to use the first method. The second method mentioned has advantages which warrant a more careful study of its use. However, the lack of a satisfactory sand to be used as the standard of comparison was the deciding factor against the further investigation of this method at the present time.

The sieve analyses of over 200 sand samples were examined to select a grading suitable for adoption as the standard. This grading should be such that it corresponds closely with the sieve analysis of what might be termed a typical concrete sand. It should afford as true an indication as is possible of the mean hardness or resistance to abrasion of the sand grains, and should be produced without an undue amount of labor. Such a grading was established and testing of the sands was begun to determine a criterion of abrasive loss, this value to be based upon the known behavior of the material in service as well as the character of the mineral constituents.

The test is made on samples weighing 500 grams to the nearest tenth of a gram, prepared from sand graded in the following proportions:

Size of grain	Per cent
¼-inch to 10-mesh	20
10-mesh to 20-mesh	20
20-mesh to 30-mesh	25
30-mesh to 40-mesh	20
40-mesh to 50-mesh	15

The sample is placed in the standard Deval abrasion machine with an abrasive charge of ten ¾-inch steel balls and run for 2,000 revolutions at a rate of 30 to 33 revolutions per minute. At the end of the test run the sample is removed from the cylinder, weighed to check against loss, and tested on a 50-mesh sieve. The amount passing this sieve is considered the loss by abrasion and is expressed as a percentage of the original weight.

A number of concrete sands were tested in this manner and the results compared with the reported service record of the materials. These samples included several different types of sands such as sands predominating in quartz grains, sands containing a large percentage of sedimentary rock grains, and sands containing appreciable amounts of feldspar and mica. The majority of these sands were routine samples submitted by State highway departments in connection with Federal-aid road construction. Some abrasion tests were also made on these sands, using that portion passing the 20-mesh and retained on the 30-mesh sieve. Tension tests were also made on samples prepared with the same grading as was used for the graded abrasion samples in addition to the routine tension tests on the material as received.

Table 2, shows the percentage of wear, tensile-strength ratio, and mineral composition of 36 sands tested as described above. These sands show percentages of wear varying from 6 to 19.5 in the graded abrasion test, illustrating the great variation in hardness and durability of sand grains that may be encountered in actual practice. It will be noted that the sands containing limestone, sandstone, feldspar, or mica generally have a high percentage of wear.

TABLE 2.—*Results of abrasion tests on graded sands arranged in order of descending percentages of wear*

Sample No.	Percentage of wear		Tensile strength ratio at 28 days		Mineral composition
	Graded (¼-inch–No. 50)	One-sized grading (No. 20–No. 30)	Natural grading	Prepared grading (¼-inch–No. 50)	
33	19.5		123	116	Quartz, chert, limestone.
31	18.9		119	116	Quartz, chert, sandstone, limestone.
30	18.2		137	113	Limestone and quartz.
32	17.5		113	130	Quartz, chert, limestone.
28	16.4		106	105	Quartz and sandstone.
18	16.0	8.5	113	112	Quartz and limestone.
29	14.6		98	105	Quartz, sandstone, limestone.
16	14.2	6.5	145	115	Limestone, quartz, sandstone, chert.
34	13.2		106	107	Quartz, chert, limestone.
35	12.2		129	130	Quartz, chert, sandstone, limestone.
25	12.2		147	121	Limestone, chert, quartz.
7	11.7	6.6	89	76	Quartz, feldspar, mica, granite, sandstone.
17	11.3	5.0	136	112	Quartz, chert, sandstone, limestone.
27	11.3		122	107	Quartz, limestone, feldspar.
8	10.9	5.3	102	94	Quartz, feldspar, mica.
21	10.5	6.7	127	107	Quartz, chert, limestone, sandstone.
14	9.8	2.2	109	89	Quartz and chert.
19	9.6	5.7	100	104	Quartz, chert, sandstone, limestone.
20	9.3	6.0	110	89	Do.
3	9.2	7.1	128	98	Quartz.
26	9.2		155		Limestone, quartz, shale.
5	9.1	3.7	99	99	Quartz, feldspar, chert, limestone.
2	8.8	4.1	118	108	Quartz, with some feldspar.
11	8.6	4.8	86	62	Quartz, feldspar, mica.
23	8.5	3.5	134	100	Quartz, mica, feldspar.
36	8.0		104	99	Quartz, feldspar, granite, limestone
24	8.0	2.9	82	101	Quartz.
13	7.7	3.5	102	84	Quartz and chert.
12	7.6	3.1	104	85	Do.
1	7.0	3.3	128	99	Quartz.
9	7.0	3.1	130	100	Quartz and chert.
10	7.0	2.1	103		Quartz.
4	6.5	2.5	96	104	Quartz and sandstone.
6	6.5	2.2	119	113	Quartz.
15	6.5	2.9	109	90	Quartz, chert, feldspar, granite.
22	6.0	2.8	147	102	Quartz and some chert.

Some of the samples show both a high percentage of wear and a high tensile-strength ratio. The high-tensile strength is due, without doubt, to the coarse grading of the sample, and the abrasion test furnishes the means of guarding against misinterpretation of such results.

No relationship is found between the results of the abrasion test for the graded samples and those for the one-sized samples, except that the latter is always less. This further demonstrates the necessity of representing the entire coarse material in the test samples. Nor does there appear to be any relation between the test results for the graded samples and the results of tension tests made on artificially graded samples. Although the effect of grading has been eliminated in these tension tests the results are still affected by the shape, surface condition, absorption, and mineral composition of the grains, whereas the abrasion test is affected mainly by the mineral composition.[3]

ADVANTAGES OF PROPOSED TEST DISCUSSED

The abrasion test is proposed as a direct test for quality of sand grains. It is not sufficient by itself to determine the suitability of a sand for use in concrete, but should be used rather as a supplementary test. To test a sand for its suitability for use in concrete, a mechanical analysis should be made to determine the grading, a washing test to determine the quantity of silt and clay, a color test to determine the presence of organic compounds, a strength test to determine if the clay or organic compounds have a deleterious effect upon the binding properties of the cement, and an abrasion test to determine if the sand grains are of sufficient strength and durability. These tests will furnish complete data regarding the suitability of a sand, both as to size and quality.

In a recent routine investigation of sand made by the Bureau of Public Roads it was found that the resistance of mortar to failure through freezing is in general agreement with the percentage of wear of the sands used when the gradings of the sands were approximately the same. The results were as follows:

Sample No.	Percentage of wear	Reduction in compressive strength of 1:2 mortar after 20 freezings and thawings
		Per cent
18	8.0	0
94	11.3	2
17	12.2	3
16	13.2	8
9	14.6	8
95	16.5	9
12	17.5	11
10	18.2	5
11	18.4	11
15	19.5	8

[3] Limited tests fail to demonstrate that the shape of grain causes an appreciable variation in the loss by abrasion.

The chief advantages of this abrasion test are as follows:

It is a direct measure of the quality of the sand grains.

The effect of grading is eliminated.

It is almost entirely free from the personal equation of the operator.

It furnishes a determination of the quality of a sand within a few hours.

Duplicate tests check each other very closely. The mean variation between individual tests of the same material should not generally be more than 5 per cent of the average.

The grading used approximates that of normal concrete sands and samples usually may be prepared with a minimum of labor and material.

The choice of a criterion to gauge the results has been given attention. Comparing abrasion test results with reports by field engineers on service behavior it appears that a percentage of wear of 9 may be considered as the limit beyond which a sand should not be classified as excellent. The selection of a sand will, of course, be tempered by local conditions such as the availability of other sand, the general type of sand, and the purpose for which it is used. For example, in localities where the sands contain a large percentage of sedimentary rock grains a much higher limit must be allowed. As a general rule, however, a clean, well-graded sand having an abrasion loss of 9 or less, when tested as described above, should prove satisfactory for use in concrete pavements.

REPORT ON PLAN OF HIGHWAY IMPROVEMENT FOR CLEVELAND REGIONAL AREA NOW AVAILABLE

The report of a plan of highway improvement in the regional area of Cleveland by the Bureau of Public roads and the County Commissioners of Cuyahoga County is now available for distribution. This report should be of particular interest to those connected with the planning of future highway development in and around urban areas. In many cases it will probably serve as a model in conducting similar work.

The investigation was undertaken in order to obtain essential facts concerning traffic and its distribution on the highways of the regional area, and the condition of present highway surfaces, structures, and railroad crossings at grade, as a basis for planning the development of new arterial highways, the reconstruction and widening of present surfaces and structures, and the separation of railroad grade crossings, to serve present and expected future traffic during a period of 10 years.

The first part of the report contains a summary of the principal conclusions, the second the detailed data of the survey upon which the findings are based, and the third the plan of highway improvement.

Features of special interest are the studies of the transverse distribution of traffic on roadways as affected by highway conditions and studies of the effect on speed, of traffic density, intersections, and other factors.

Copies of the report may be secured by application to the Bureau of Public Roads.

C

ROAD PUBLICATIONS OF BUREAU OF PUBLIC ROADS

Applicants are urgently requested to ask only for those publications in which they are particularly interested. The Department can not undertake to supply complete sets nor to send free more than one copy of any publication to any one person. The editions of some of the publications are necessarily limited, and when the Department's free supply is exhausted and no funds are available for procuring additional copies, applicants are referred to the Superintendent of Documents, Government Printing Office, this city, who has them for sale at a nominal price, under the law of January 12, 1895. Those publications in this list, the Department supply of which is exhausted, can only be secured by purchase from the Superintendent of Documents, who is not authorized to furnish publications free.

ANNUAL REPORTS

Report of the Chief of the Bureau of Public Roads, 1924.
Report of the Chief of the Bureau of Public Roads, 1925.
Report of the Chief of the Bureau of Public Roads, 1927.
Report of the Chief of the Bureau of Public Roads, 1928.

DEPARTMENT BULLETINS

No. 105D. Progress Report of Experiments in Dust Prevention and Road Preservation, 1913.
*136D. Highway Bonds. 20c.
220D. Road Models.
257D. Progress Report of Experiments in Dust Prevention and Road Preservation, 1914.
*314D. Methods for the Examination of Bituminous Road Materials. 10c.
*347D. Methods for the Determination of the Physical Properties of Road-Building Rock. 10c.
*370D. The Results of Physical Tests of Road-Building Rock. 15c.
386D. Public Road Mileage and Revenues in the Middle Atlantic States, 1914.
387D. Public Road Mileage and Revenues in the Southern States, 1914.
388D. Public Road Mileage and Revenues in the New England States, 1914.
390D. Public Road Mileage and Revenues in the United States, 1914. A Summary.
407D. Progress Reports of Experiments in Dust Prevention and Road Preservation, 1915.
463D. Earth, Sand-clay, and Gravel Roads.
*532D. The Expansion and Contraction of Concrete and Concrete Roads. 10c.
*537D. The Results of Physical Tests of Road-Building Rock in 1916, Including all Compression Tests. 5c.
*583D. Reports on Experimental Convict Road Camp, Fulton County, Ga. 25c.
*660D. Highway Cost Keeping. 10c.
*670D. The Results of Physical Tests of Road-Building Rock in 1916 and 1917. 5c.
*691D. Typical Specifications for Bituminous Road Materials. 10c.
*724D. Drainage Methods and Foundations for County Roads. 20c.
*1077D. Portland Cement Concrete Roads. 15c.
1216D. Tentative Standard Methods of Sampling and Testing Highway Materials, adopted by the American Association of State Highway Officials and approved by the Secretary of Agriculture for use in connection with Federal-aid road construction.
1259D. Standard Specifications for Steel Highway Bridges, adopted by the American Association of State Highway Officials and approved by the Secretary of Agriculture for use in connection with Federal-aid road work.

DEPARTMENT BULLETINS—Continued

No. 1279D. Rural Highway Mileage, Income, and Expenditures, 1921 and 1922.
1486D. Highway Bridge Location.

DEPARTMENT CIRCULARS

No. 94C. T. N. T. as a Blasting Explosive.
331C. Standard Specifications for Corrugated Metal Pipe Culverts.

TECHNICAL BULLETIN

No. 55. Highway Bridge Surveys.

MISCELLANEOUS CIRCULARS

No. 62M. Standards Governing Plans, Specifications, Contract Forms, and Estimates for Federal Aid Highway Projects.
93M. Direct Production Costs of Broken Stone.
109M. Federal Legislation and Regulations Relating to the Improvement of Federal-aid Roads and National-Forest Roads and Trails.

FARMERS' BULLETIN

No. *338F. Macadam Roads. 5c.

SEPARATE REPRINTS FROM THE YEARBOOK

No. 914Y. Highways and Highway Transportation.
937Y. Miscellaneous Agricultural Statistics.

TRANSPORTATION SURVEY REPORTS

Report of a Survey of Transportation on the State Highway System of Connecticut.
Report of a Survey of Transportation on the State Highway System of Ohio.
Report of a Survey of Transportation on the State Highways of Vermont.
Report of a Survey of Transportation on the State Highways of New Hampshire.
Report of a Plan of Highway Improvement in the Regional Area of Cleveland, Ohio.

REPRINTS FROM THE JOURNAL OF AGRICULTURAL RESEARCH

Vol. 5, No. 17, D- 2. Effect of Controllable Variables upon the Penetration Test for Asphalts and Asphalt Cements.
Vol. 5, No. 19, D- 3. Relation Between Properties of Hardness and Toughness of Road-Building Rock.
Vol. 5, No. 24, D- 6. A New Penetration Needle for Use in Testing Bituminous Materials.
Vol. 6, No. 6, D- 8. Tests of Three Large-Sized Reinforced-Concrete Slabs Under Concentrated Loading.
Vol. 11, No. 10, D-15. Tests of a Large-Sized Reinforced-Concrete Slab Subjected to Eccentric Concentrated Loads.

* Department supply exhausted.

UNITED STATES DEPARTMENT OF AGRICULTURE

BUREAU OF PUBLIC ROADS

CURRENT STATUS OF FEDERAL AID ROAD CONSTRUCTION

AS OF

DECEMBER 31,1928

STATE	COMPLETED MILEAGE	UNDER CONSTRUCTION					APPROVED FOR CONSTRUCTION					BALANCE OF FEDERAL-AID FUNDS AVAILABLE FOR NEW PROJECTS	STATE
		Estimated total cost	Federal aid allotted	MILEAGE			Estimated total cost	Federal aid allotted	MILEAGE				
				Initial	Stage[1]	Total			Initial	Stage[1]	Total		
Alabama	1,902.0	$ 3,245,575.94	$ 1,619,227.38	249.1	12.3	261.4	$ 936,130.03	$ 468,065.00	29.9	21.1	51.0	$ 2,519,324.79	Alabama
Arizona	877.2	1,460,664.47	1,232,991.67	70.8	9.6	80.4	160,164.56	43,021.41		4.4	4.4	3,717,102.10	Arizona
Arkansas	1,736.3	3,742,844.14	1,656,719.01	102.4	6.6	109.0	74,477.68	37,238.83	10.9		10.9	3,051,061.11	Arkansas
California	1,523.7	9,149,190.75	4,218,315.03	233.1	.6	233.7	1,752,374.93	903,973.32	71.6	.1	71.7	3,107,061.68	California
Colorado	1,063.7	3,461,340.88	1,863,064.00	156.8	15.0	171.8	321,702.70	180,559.84	17.3	.9	18.2	3,042,624.51	Colorado
Connecticut	220.1	1,893,291.22	419,866.53	21.7		21.7	667,713.84	279,338.73	3.6		3.6	837,708.90	Connecticut
Delaware	205.3	534,288.82	255,507.30	15.7		15.7						460,890.72	Delaware
Florida	429.5	2,783,853.47	1,232,677.16	110.7	5.5	116.2						2,066,457.57	Florida
Georgia	2,456.7	5,435,922.73	2,512,656.92	249.7	46.6	296.3	259,439.89	124,002.22	13.4	4.6	18.0	1,995,062.27	Georgia
Idaho	1,077.2	1,836,484.93	1,096,040.57	128.5	10.8	139.3	70,186.67	41,816.95	3.8		3.8	1,001,180.03	Idaho
Illinois	1,777.8	20,268,114.90	9,218,013.47	635.3		635.3	1,538,554.77	648,267.00	38.8		38.8	3,112,847.70	Illinois
Indiana	1,243.6	5,832,583.76	2,786,312.46	175.2	3.5	178.7	997,285.77	432,728.13	32.5		32.5	1,959,718.95	Indiana
Iowa	2,995.3	2,525,321.36	1,005,108.23	44.4	81.8	126.2	562,850.93	256,968.32	14.6	22.5	37.1	2,075,430.98	Iowa
Kansas	2,344.6	6,262,048.53	2,521,985.75	369.4	16.3	385.7	546,597.76	180,516.90	39.2		39.2	2,138,351.92	Kansas
Kentucky	1,258.6	4,934,089.81	2,214,736.98	219.6		219.6	789,026.85	325,213.41	47.3		47.3	1,425,692.86	Kentucky
Louisiana	1,281.2	4,681,926.40	2,332,944.70	193.2		193.2	103,055.30	25,000.00	.2		.2	1,209,402.36	Louisiana
Maine	466.3	2,245,679.85	749,696.01	52.9		52.9	192,121.39	93,601.55	8.9		8.9	1,452,991.86	Maine
Maryland	557.6	1,742,202.42	799,750.00	70.4	7.2	77.6						664,211.23	Maryland
Massachusetts	567.7	2,827,192.55	897,122.74	49.4		49.4	738,843.93	190,800.00	12.8		12.8	2,410,618.43	Massachusetts
Michigan	1,441.3	11,180,946.36	4,723,846.96	272.4		272.4	779,320.00	324,456.86	14.1	6.5	20.6	2,163,236.82	Michigan
Minnesota	4,089.8	1,083,279.54	335,618.27	96.0	11.2	107.2	165,941.21	15,000.00	.1		.1	2,147,297.96	Minnesota
Mississippi	1,591.1	5,261,484.71	2,413,698.27	229.7	41.5	271.2	290,009.59	145,004.78	19.6		19.6	1,457,152.13	Mississippi
Missouri	2,280.2	7,657,880.05	2,885,886.21	167.5	48.3	215.8	1,465,671.69	635,888.93	43.7	17.0	60.7	1,816,318.71	Missouri
Montana	1,518.1	3,239,591.90	1,981,891.64	241.4	13.4	254.8	716,003.35	376,464.83	79.6	.2	79.8	5,514,866.55	Montana
Nebraska	3,462.1	3,735,878.57	1,846,603.33	341.8	106.0	447.8	330,285.16	164,142.54	7.2	28.4	35.6	3,394,162.30	Nebraska
Nevada	1,002.3	1,281,390.29	1,115,874.66	141.7	69.4	211.1	181,620.00	161,341.93	34.5	1.6	36.1	1,084,980.62	Nevada
New Hampshire	331.7	279,253.01	108,613.31	7.5		7.5						399,082.40	New Hampshire
New Jersey	442.9	5,225,494.22	907,122.35	60.8		60.8	108,429.58	33,975.00	2.3		2.3	945,629.94	New Jersey
New Mexico	1,786.4	3,255,434.56	2,130,101.96	202.3		202.3	278,971.64	176,951.68	22.9	5.1	28.0	1,346,859.13	New Mexico
New York	2,034.0	28,763,300.00	6,340,585.89	422.2		422.2	1,890,931.43	383,205.00	25.6		25.6	6,981,245.33	New York
North Carolina	1,666.3	1,999,428.22	1,014,875.43	87.0	11.2	98.2	509,931.33	251,075.56	14.4	7.2	21.6	1,889,148.08	North Carolina
North Dakota	3,678.0	2,794,228.69	1,209,991.02	419.5	94.5	514.0	882,876.79	301,186.37	151.7	112.8	264.5	1,239,607.96	North Dakota
Ohio	1,960.2	10,899,160.39	3,852,368.15	238.4	.1	238.5	3,997,080.00	1,167,745.00	55.1	9.8	64.9	3,548,848.06	Ohio
Oklahoma	1,703.5	3,330,275.31	1,519,966.41	143.7	32.5	176.2	549,239.88	247,686.84	15.4	8.5	23.9	1,673,342.95	Oklahoma
Oregon	1,132.5	549,965.57	322,322.32	31.9		31.9	108,443.50	67,484.39	.2		.2	2,344,038.92	Oregon
Pennsylvania	1,995.6	13,140,034.43	3,504,428.43	211.1	14.1	225.2	1,708,007.20	567,923.88	35.2		35.2	3,633,166.51	Pennsylvania
Rhode Island	159.6	610,898.36	153,054.55	8.8		8.8	381,212.36	149,805.00	10.0		10.0	776,149.23	Rhode Island
South Carolina	1,715.8	6,804,078.45	1,488,452.17	159.3	88.1	247.4	3,046.08	1,000.00	1.1		1.1	1,077,107.90	South Carolina
South Dakota	3,233.6	2,340,629.80	1,272,859.49	421.5	43.3	464.8	245,331.08	134,932.07	18.1	3.0	21.1	1,364,147.77	South Dakota
Tennessee	1,067.7	4,708,684.21	2,103,133.51	111.9	60.6	172.5	541,047.98	246,457.86		24.4	24.4	2,114,787.78	Tennessee
Texas	6,076.7	10,930,270.08	4,626,100.95	414.2	158.0	572.2	6,195,218.22	2,632,724.32	231.8	131.5	363.3	5,166,360.01	Texas
Utah	898.7	1,347,246.19	885,064.05	64.8	4.0	68.8	123,239.39	91,197.14	6.6		6.6	904,551.79	Utah
Vermont	228.9	965,465.68	288,777.15	20.5		20.5						409,935.95	Vermont
Virginia	1,313.4	3,662,257.11	1,114,862.93	93.1	15.2	108.3	643,617.27	20,749.23	22.0		22.0	1,450,366.97	Virginia
Washington	829.7	3,895,685.06	1,313,775.25	74.5	18.1	92.6	82,670.11	44,000.00	4.7		4.7	1,537,637.83	Washington
West Virginia	691.7	1,172,976.95	551,151.17	46.6	2.5	49.1	471,311.61	210,674.18	11.2	9.9	21.1	1,102,671.28	West Virginia
Wisconsin	2,107.6	4,121,355.56	1,796,925.96	124.0	4.9	128.9	74,197.72	37,088.00	6.1		6.1	3,180,757.66	Wisconsin
Wyoming	1,610.7	1,374,164.03	844,966.46	159.2	.4	159.6						1,029,176.31	Wyoming
Hawaii	39.4	175,931.99	57,501.20	1.8		1.8						1,432,123.59	Hawaii
TOTALS	76,074.9	230,649,286.22	91,343,164.36	8,163.4	1,053.1	9,216.5	32,434,181.17	12,819,273.00	1,178.0	419.5	1,597.5	101,372,498.41	TOTALS

[1]The term stage construction refers to additional work done on projects previously improved with Federal aid. In general, such additional work consists of the construction of a surface of higher type than was provided in the initial improvement.